

3.0 FREE SURFACE AIR ENTRAINMENT ON SPILLWAYS

I R Wood*

* Professor of Civil Engineering, University of Canterbury,
Christchurch, New Zealand

3.1 Introduction

The flow down a long spillway can be divided into a number of distinct regions [Figs. 3.1 & 3.2]. In the non aerated region close to the spillway crest the boundary layer grows from the spillway floor. Outside the boundary layer the flow is predominantly irrotational and the water surface is smooth and glassy. Any air that is entrained in this region will come from disturbances generated by vorticity in the reservoir. These disturbances appear as longitudinal streaks of air entrainment on the spillway (Fig. 3.1) and although important in interpreting prototype measurements they do not affect the spillway design.

At the point where the boundary layer reaches the free surface the surface becomes disturbed and entrainment by the multitude of vortices in the turbulent flow commences. This point has been called the point of inception. However, the outer edge of the boundary layer is irregular, (Fig. 3.2b) and this is reflected in the variation of the first appearance of turbulence on the water surface. The first appearance of turbulence has been detected in the laboratory by using stroboscopic lights to observe the change in the surface roughness (Gangadharaiah et al, 1970). Govinda Rao et al (1961); Hino (1961); Gangadharaiah et al (1970) and Rao et al (1973) have written on the energy required in the turbulent eddies to ensure air entrainment. However on a prototype spillway the energy is always sufficient, and, once the turbulence in the boundary layer reaches the surface, entrainment commences. This may be observed

in Fig. 3.1 where the longitudinal streaks of white water are caused by the reservoir disturbances. The more general irregular first bursts of turbulence indicate the start of more general air entrainment.

Downstream of the start of air entrainment a layer containing a mixture of both air and water gradually extends through the flowing fluid. Its rate of growth is small, and normal boundary layer approximations are appropriate. For small slopes, equilibrium is established before the air water mixture reaches the spillway floor. However, for steep slopes air reaches the lower boundary (Fig. 3.2). Measurements in the mixed layer by Cain (1978) show that the air water mixture has a highly irregular wavy surface in which overturning waves and the return of water droplets ejected from the surface [Volkart, 1980] continuously entrain air (Fig. 3.3). This air is broken into bubbles which are dispersed by the intense turbulence. The flow near the surface has a high concentration of air frequently in the range of 0.5 - 0.9. The largest bubbles within the surface region are 10 - 20 mm in diameter. Away from the surface the flow is likely to be less aerated with bubbles being broken down by the shear to a diameter of 0.5 - 3 mm. These sizes are thought to result from an equilibrium between the agitation of the flow and the bubble resistance to deformation due to its surface tension.

Above the wavy but more or less continuous interface between the air and air-water, water droplets of various sizes are present. Indeed the spray projected from the surface may extend to a considerable height above the main flow. However it contributes little to the total discharge.

Far downstream from the point of inception the flow becomes uniform (Fig. 3.2a). Thus the air concentration along with the other open channel flow properties does not vary with distance. In between the uniform flow region and the point of inception there is a gradually varied flow region.

A knowledge of the air concentration at positions down the spillway is important to the designer as it affects:

- the increase in the depth for which additional freeboard must be provided,
- the point at which the region with entrained air reaches the spillway floor,
- the inlet conditions for the design of any dissipator downstream of the spillway.

The air next to the floor has two effects:

- The fluid becomes compressible and the possibility of cavitation damage is greatly reduced. Above this point the fluid is essentially incompressible, and if the velocities are large enough, cavitation will occur.
- The air next to the surface reduces the effective shear stress and hence the local friction factor. This implies a greater velocity of the flow than would otherwise occur.

3.2 The Point of Inception of Air Entrainment

The flow in the non-aerated region has been discussed by Michels and Lovely (1953), Bauer (1954), Halbronn (1954), Campbell, Cox and Boyd (1965), Cassidy (1966), Rao and Kobus (1973), Keller and Rastogi (1971, 1977) and Wood, Ackers and Loveless (1983). In these studies the interest was in the mean distance x_I from the start of the growth of the boundary layer over the crest to where it reaches the free surface, as shown in Fig. 3.2. The distance to the point of inception x_I (Fig. 3.2a) and the properties of the point of inception [the maximum velocity u_I and the depth d_I] are a function of the spillway slope and the conditions at the dam crest. These may be the head above the dam crest (h) or the discharge over the dam [$q \text{ m}^3/\text{ms}$]. It is convenient to use q and to use a length scale d_{cs} defined as $[q^2/g \sin\theta]^{1/3}$.

For prototype flows the Reynolds and Weber numbers can be neglected and there are no pressure gradients. The dimensional analysis of Chapter 1 can then be written as

$$\frac{x_I}{d_{cs}}, \frac{d_I}{d_{cs}}, \frac{u_I d_{cs}}{q} = \phi \left[\frac{d_{cs}}{k_s}, \theta, \text{geometric values} \right]$$

where θ is the spillway slope.

The work of Campbell et al (1965), Cassidy (1966), Rao and Kobus (1973) and Keller and Rastogi (1971, 1977) applies to an ungated crest designed to the specification of the United States Army Corps of Engineers and thus takes into account the geometry of this particular crest. Bauer (1954) and Halbronn(1954) neglected the effect of the spillway crest geometry by assuming that the length of the spillway surface over which the developing boundary grows approximates the slope distance x_s (defined as in Fig. 3.2). This approximation is acceptable provided the point of inception of air entrainment is far enough down the spillway (i.e. provided $x_I/a \gg 1$ where a is a typical crest dimension). Under these conditions Halbronn and Bauer show that the experimental results should have the form

$$\frac{\delta}{x_s} = \alpha \left[\frac{x_s}{k_s} \right]^{-\beta} \quad 3.2.2$$

where δ is the boundary layer thickness defined as the perpendicular distance from the surface to where the velocity is 99% of its irrotational value ($0.99 u_{fs}$ where u_{fs} is the free streamline velocity). Boundary layer analysis indicated that the value of α and β are of order 0.03 and 0.14 respectively. At the traditional point of inception of the air entrainment the value of the boundary layer thickness is approximately d_I .

If at these distances down the spillway, Bauer's approach is used and the velocity distribution is approximated by

$$u/u_{fs} = (y/\delta)^{1/n} \quad 3.2.3$$

then at the point of inception u_{fs} will equal the surface velocity u_I , and δ will equal d_I and equations 3.2.2 and 3.2.3 may be combined with Bernoulli's equation to yield

$$\frac{x_s}{d_{cs}} = K_1^{2K_2/\beta} \left[\frac{d_{cs}}{k_s} \right]^{2K_2} \quad 3.2.4$$

and

$$\left[\frac{U_I}{2gd_{cs}} \right]^{0.5} = K_1^{K_2/\beta} [\sin\theta]^{0.5} \left[\frac{d_{cs}}{k_s} \right]^{K_2} \quad 3.2.5$$

$$\frac{d_I}{d_{cs}} = \alpha K_1 \left(1 - K_2/\beta \right) \left[\frac{d_{cs}}{k_s} \right]^{-K_2} \quad 3.2.6$$

where $K_1 = \left(\frac{n+1}{\alpha n \sqrt{2}} \right)$ and $K_2 = \frac{\beta}{3-2\beta}$

The terms in the equations are all design parameters and enable the direct computation of the position and properties at the inception point. From these expressions and the order of magnitude of β and n , all the inception point values depend only slightly on k_s and n . To use these results one must select exact values of α , β and n , and indeed Halbronn (1954) and Bauer (1954) suggest values. However Keller and Rastogi (1971, 1977) used a mathematical model based on the two dimensional form of the time-averaged Navier Stokes equation to compute the developing boundary layer and its intersection with the free surface. To solve the equations and hence to calculate the point of inception, the pressure was assumed to vary linearly in the direction perpendicular to the spillway face and the Reynolds stress was computed using a number of empirical but universal constants. Their computed data for slopes between 5° and 70° and for the variables contained in equation 3.2.4 is plotted in Fig. 3.4. From the slope of the lines on this figure we get $K_2 = 0.035$ [$\beta = 0.1$] and

$$K_1 = 39 [\sin\theta]^{0.11} \quad 3.2.7$$

This with the value of n of 6.4 from Cains (1978) data give

$$\alpha = 0.021 [\sin\theta]^{-0.11} \quad 3.2.8$$

Substituting these values into the equations gives a direct method

of computing the point of inception for a standard ungated spillway. These equations are given in Fig. 3.4. Eliminating d_{cs} from these equations and using $\sin\theta = h_s/x$ yields

$$\frac{d_I}{x_s} = \frac{\delta}{x_s} = 0.021 \left[\frac{x_s}{h_s} \right]^{0.11} \left[\frac{k_s}{x_s} \right]^{+0.10} \quad 3.2.9$$

This new form of the boundary layer equation is applicable for slopes of 5° to 70° and is useful because it shows the relative importance of the factors which influence boundary layer growth on the accelerating region of the spillways. Thus the boundary layer thickens basically in proportion to distance, x , it is increased in thickness by greater roughness, k_s , and is reduced by the velocity change down the spillway [quantified in the terms containing h_s]. This equation holds only on a standard spillway. However on a spillway of constant width and gradually varying slope the boundary layer will be approximately in local equilibrium and the boundary layer growth rate can be obtained by differentiating 3.2.9 giving

$$\frac{d\delta}{dx} = \frac{\delta}{x} \left[0.9 - 0.11 x \cot\theta \frac{d\theta}{dx} \right] \quad *3.2.10$$

The discharge within the boundary layer is then obtained as

$$q_\delta = \frac{n}{n+1} \sqrt{2gh_s \delta} \quad 3.2.11$$

where n comes from the velocity distribution within the boundary layer (3.2.3). The total depth of the flow can then be computed by using the Bernoulli equation to compute the velocity outside the boundary layer [u_{fs}] and then using

$$d = \delta + (q - q_\delta)/u_{fs} \quad 3.2.12$$

* This equation may also be modified to allow for a gradual variation in width (Appendix 3.1).

If the first reach of the boundary layer development can approximate that of standard crest, at a constant angle, then equation 3.2.10 can be used to compute the first boundary layer depth. Subsequent numerical calculations using equations 3.2.10, 3.2.12, do not depend on a constant spillway slope and enable the point of inception to be determined on any spillway chute.

The traditional point of inception occurs when discharge in the boundary layer (q_δ) equals the spillway discharge. However, as the outer edge of the boundary layer is very irregular and ranges between 0.4 and 1.2 times its calculated depth (Daily & Harleman 1966) air entrainment will sometimes commence upstream of its traditional point and there will sometimes be positions without air entrainment downstream of the traditional inception point. This large variation makes the interpretation of the very few observations of the point of inception extremely difficult.

For an estimate of the first occurrence of air entrainment it is necessary to carry the calculations forward into the air entraining region and the best estimate is obtained if the calculations are carried forward until the flow up to this outer edge of the boundary layer equals the total flow, i.e.

$$q = q_{1.2\delta} = \frac{(6n + 1)}{5(n + 1)} \sqrt{2gh_s \delta} \quad 3.2.13$$

where $q_{1.2\delta}$ is the discharge at 1.2 times the boundary layer thickness from the spillway floor.

3.3 The Properties of the Flow Downstream of the Point of Inception

3.3.1 Introduction

In all the air containing regions the local air concentration c is defined as the volume of air per unit volume and this will normally be taken as a time averaged value. The equivalent clear water depth is then

$$d = \int_0^{\infty} (1 - c) dy \quad 3.3.0$$

where y is measured perpendicular to the spillway surface. An average water velocity is then

$$u_v = q/d \quad 3.3.1$$

where q is the spillway water discharge per unit width. A characteristic depth for the self-aerated flow is defined for both model and prototype measurements as that depth where the average air concentration is 90% ($y_{.9}$).

The mean air concentration averaged over this characteristic depth may then be defined from

$$(1 - \bar{c})y_{.9} = d \quad 3.3.2$$

A characteristic water velocity ($u_{.9}$) is defined as that at $y_{.9}$.

3.3.2 The uniform flow equilibrium air concentration region

This region is the simplest of those that occur and will be dealt with first. As in the uniform flow region of a normal open channel the mean properties of the flow, such as its depth (d_e or $y_{.9e}$), and the depth averaged air concentration (\bar{c}_e) can only depend on the spillway discharge/unit width, its slope (and the component of gravity down the slope gS or $g\sin\theta$), the roughness and the fluid properties. This leads to

$$\bar{c}_e, \frac{8gSd_e^3}{q^2} = \phi \left[\frac{q}{\nu}, \frac{d}{k_s}, S \right] \quad 3.3.3$$

or

$$\bar{c}_e, f_e = \phi \left[\frac{q}{\nu}, \frac{d}{k_s}, S \right] \quad 3.3.4$$

where f_e is the friction factor for the region of uniform flow.

For all the flows discussed the Reynolds number effects will be small and we have only a limited range of roughness. Thus to an acceptable approximation

$$\bar{c}_e, f_e = \phi[S] \quad 3.3.5$$

Similarly for the air concentration and velocity distributions we have

$$c, \frac{u}{u_{.9}} = \phi \left[\frac{y}{y_{.9}} \right] \quad 3.3.6$$

The classic set of aerated flow measurements are those published by Straub and Anderson (1958) for the region of uniform flow. They measured the discharge, the air concentration and the velocity in a flume 15.25 m (50 ft) long, 0.46 m (1.5 ft) wide and 0.30 m (1.0 ft) deep that was roughened to enhance air entrainment. They were able to vary the slope and the discharge independently and obtained air concentration distributions for slopes of from 7.5° to 75° and for discharges from 0.136 m²/sec (1.47 ft²/sec) to 0.927 m²/s (10 ft²/sec). Anderson's measurements were of air concentrations on the flume centreline 13.73 m (45 ft) from the flume inlet for flows which appeared to be in the equilibrium region. Equilibrium flow was considered to be "that condition of the flow of the air-water mixture for which the air-concentration distribution was the same at two sections 3.05 m (10 ft) apart along the channel. This condition could be obtained by the adjustment of the initial depth of flow through control of the inlet-gate opening. Repeated measurements of the profiles were made at the two sections for different gate openings until the two air-concentration profiles were similar. Comparisons were made of the concentration at corresponding distances normal to the bed". Other results reported by Rao et al. (1973) are similar to those obtained by Straub and Anderson. In this case however the tabulated results were not published. The mean air concentrations defined by 3.3.3 have been computed from Straub and Anderson's results and are plotted as a function of discharge in Fig. 3.5. The Figure shows that for each slope there is a region where \bar{c}_e does not vary with discharge and a region where \bar{c}_e decreases with increasing discharge. [For some of the small slopes this second region does not exist.] Equation 3.3.5 suggests that in the equilibrium region \bar{c}_e would be independent of the discharge and Figure 3.5 may therefore be divided into a region which satisfies equation 3.35 [the uniform flow

region] and a region in which this equation is not satisfied [the gradually varied flow region].

Similarly if the air concentration distribution is plotted in the form of equation 3.36 then only the data in the equilibrium region satisfies this equation. This is illustrated in Figure 3.6. This figure is for the 45° slope and shows that only for the smaller discharges [0.136 - 0.396 m²/sec] is the single curve predicted by equation 3.37 obtained. The curves for larger discharges are similar to those obtained in the gradually varied flow region of Aviemore spillway (Fig. 3.7). Indeed the data for the larger discharges can be interpreted as data obtained at distances close to the point of inception. Curves similar to those obtained in Fig. 3.6 are obtained for slopes of 22.5°, 30°, 35.7°, 60°, 75° (Appendix 3.2, Figures 3.2.3 - 3.2.7) but for smaller slopes of 7.5° and 15° all the flows appear to be in equilibrium (Appendix 3.2, Figures 3.2.1 and 3.2.2).

The region where the air concentration is gradually varied is one of very slow growth and in spite of the quality and care, measurements only three metres apart could have been interpreted as being in the uniform flow region even though our later examination suggests that they were not. The mean equilibrium air concentration is plotted as a function of slope in Fig. 3.8. Finally the distribution of the equilibrium air concentration for all slopes is plotted in Fig. 3.9.

An analytic solution for the form of the curves in Fig 3.9 can be obtained by use of a simple physical model that is analogous to that used for the distribution of suspended sediment in a flowing stream. (Appendix 3.3)

3.3.3 The Friction Factor

As Fig. 3.8 shows for Straub and Anderson's data the equilibrium air concentration is a unique function of the spillway slope. Thus equation 3.3.6 may be written as

$$f_e = \phi \left(\bar{c}_e \right) \quad 3.3.7$$

and the data is plotted in this form in Fig. 3.10. Further, great care was taken in their experiments to ensure that the change in air concentration between the sections was very small. Thus although the evidence is that the final mean air concentration was not always reached the slope of the total energy line must be very nearly parallel to the bed slope. Thus all of their points are included in the calculations of the friction factor.

The value of f_e is constant until the mean air concentration reaches 30 %. At this point the air concentration at the spillway floor is approximately 5% and as the air concentration increases the value of f_e falls rapidly.

No direct information is available on the manner in which f_e varies with roughness. However if eqn 3.3.8 is written in the form

$$f_e = \phi \left[\frac{d_e}{k_s} \right] \phi_2 \left(\bar{c}_e \right) \quad 3.3.8$$

and use is made of the limit that when $\bar{c}_e = 0$, $f_e = f$ we get

$$\frac{f_e}{f} = \phi_2 \left(\bar{c}_e \right) \quad 3.3.9$$

This scale is also plotted in Fig. 3.10.

3.3.4 The Velocity Distribution

The velocities appropriate to the flow of an air water mixture are the water velocity, u , the air velocity, u_a , and the mixture velocity defined by

$$u_m \rho_m = \rho_w u (1 - c) + \rho_a u_a c \quad 3.3.10$$

where

$$\rho_m = \rho_w [1 - c] + \rho_a c$$

In the upper region of the air water mixture the air flow is being driven by the drag of the projected water droplets and u_a will be less than u . In the major part of the air water mixture the air bubbles will be

surrounded by water and because of their relatively small density their velocity in the direction down the spillway will be close to the water velocity.

Cain (1978) used an electronic probe which gave a signal when it was in water and no signal when it was in air. He placed two of these probes in line a known distance apart, recorded the output from each of them separately, obtained the peak in the correlation between the two records and was then able to obtain the average velocity of the air water interfaces. This instrument gave consistent results for air concentrations of between 5 and 95%. If the velocity of these interfaces is taken as the water velocity then the velocity distribution may be written as

$$\frac{u}{u_{.9}} = \left[\frac{y}{y_{.9}} \right]^{1/6.0} \quad 3.3.11$$

and this result is independent of the mean air concentration in the range of 0 to 50%, (Fig. 3.11)(Cain and Wood, 1981). This suggests that when the rise velocity of the air bubbles is sufficiently small compared with the water velocity the velocity distribution is not affected by the air concentration. This velocity distribution is consistent with a reinterpretation of the pitot tube measurements of Lai (1971) and Viparelli (1957).

Equation 3.3.11 will be used in the subsequent analysis. No information is available about the manner in which this velocity distribution changes with large changes in the roughness parameter (d_I/k_s). However, these changes should be similar to that in a non-aerated flow.

3.3.5 Estimating the flow parameters in the uniform flow region

For any spillway slope, Fig. 3.8 gives an estimate of the mean air concentration and if the value of f without air is available then Fig. 3.10 gives the f in the air entrained flow. This enables d to be computed from $d = (q^2 f_e / 8gS)^{1/3}$. The average water velocity (u_w) is then q/d and $y_{.9}$ is $d/(1 - \bar{c}_e)$. The air concentration distribution is then obtained from

Fig. 3.9 and the water velocity distribution can be obtained from equation 3.3.11 and the fact that the Aviemore dam data shows that $u_{.9} = 1.2u_w$.

3.4 The Region of Varied Flow

3.4.1 Introduction

It remains to calculate the properties in the gradually varied flow region between the point at which air entrainment commences and the region of equilibrium flow. This requires a slightly modified equation for the gradually varied flow and an entrainment function. This latter is dealt with first.

3.4.2 The entrainment function

Between the point of inception and the uniform flow region the changes in air concentration and in the air concentration distribution are gradual. Thus, the boundary layer assumption is appropriate and for a given mean air concentration $\bar{c}(x)$ the air concentration distribution will have a shape that is close to the equilibrium air concentration. This is illustrated by a comparison of the shapes of the air concentration curves for Cain's measurements in the gradually varied flow region with the equilibrium data, Fig. 3.12. The differences are within the accuracy of the data. This suggests that the entrainment velocity v_e will be a function of local conditions only and from dimensional analysis

$$\frac{v_e}{u_{.9}} = \phi \left(Fr(x), \bar{c}(x) \right) = \beta(x) \quad 3.4.0$$

where $Fr(x)$ is the local Froude Number and $\bar{c}(x)$ is the local average air concentration. At the same time as air is being entrained, air is escaping (detrainment) and an approximate expression for the escape is $[u_r \cos\theta] \bar{c}(x)$, where u_r is the rise velocity of the bubbles.

Thus the rate of increase of the flux of air $[q_a]$ can be written as

$$\frac{dq_a}{dx} = \beta(x)u_{.9}(x) - \bar{c}(x)u_r \cos\theta \quad 3.4.1$$

If the local spillway slope is extended into the equilibrium region then in this region equation 3.4.1 becomes

$$0 = \beta_e u_{.9e} - \bar{c}_e u_r \cos\theta \quad 3.4.2$$

Subtracting equation 3.4.2 from 3.4.1

$$\frac{dq_a}{dx} = \beta(x) u_{.9(x)} - \beta_e u_{.9e} + (\bar{c}_e - \bar{c}(x)) u_r \cos\theta \quad 3.4.3$$

For $\beta(x) = \beta_e$ then this relationship satisfies the commonsense requirement for the direction of entrainment (i.e. if $u_{.9(x)} > u_{.9e}$ the first term implies a net entrainment velocity and if $\bar{c}(x) < \bar{c}_e$ we get a similar net entrainment). For a spillway on a long uniform slope the velocity variation from the point of inception to the uniform equilibrium flow is relatively small and if the first two terms in the net entrainment eqn. 3.4.3. are neglected we get

$$\frac{dq_a}{dx} = \bar{c}_e u_r \cos\theta - \bar{c}(x) u_r \cos\theta \quad 3.4.4$$

This is equivalent to assuming that the rate of entrainment of air is constant at the equilibrium value [$\bar{c}_e u_r \cos\theta$ Eqn. 3.4.2] for all points downstream of the point of inception but the rate of escape of air [$\bar{c}(x) u_r \cos\theta$] depends on the local air concentration. Firstly if it is assumed that there is no slip between the air and the water then

$$q_a = \int_0^{y_{.9}} \frac{\bar{c}}{1-\bar{c}} u \, dy \quad 3.4.5$$

Further if the velocity variation perpendicular to the spillway surface is neglected and

$$d \approx \int_0^{y_{.9}} (1-\bar{c}) \, dy = (1-\bar{c}) y_{.9} \quad 3.4.6$$

is used then equation 3.4.3 can be written as

$$q \frac{d}{dx} \left[\frac{\bar{c}(x)}{1-\bar{c}(x)} \right] = (\bar{c}_e - \bar{c}(x)) u_r \cos\theta \quad 3.4.7$$

If the x origin is taken as the point of inception and at this point the air concentration is c_v the concentration due to the longitudinal vortices,

then equation 3.4.7 may be integrated to yield equation 3.4.8 below.

$$\frac{1}{(1-\bar{c}_e)^2} \ln \left(\frac{1-\bar{c}(x)}{\bar{c}_e-\bar{c}(x)} \right) - \frac{1}{(1-\bar{c}_e)(1-\bar{c}(x))} = \frac{u_r \cos \theta}{q_v} + \frac{1}{(1-\bar{c}_e)^2} \ln \left(\frac{1-c_v}{\bar{c}_e-c_v} \right) - \frac{1}{(1-\bar{c}_e)(1-c_v)} \quad 3.4.8^*$$

From the Aviemore data the values on the left hand side of eqn 3.4.8 were computed and are plotted against x in Fig. 3.13 a and b. The data sets give straight lines with correlation coefficients of 1.00 and 0.98. This implies rise velocities of 0.39 and 0.405 m/sec. In view of the simplistic model the velocities are sufficiently close to the rise velocities of the air bubbles in still water (Fig. 1.6). Substituting the average value into equation 3.4.7 gives the general entrainment function [3.4.9]

$$q \frac{d\bar{c}}{dx} = \frac{0.4 \cos \theta}{q} (\bar{c}_e - \bar{c}(x)) (1 - \bar{c}(x))^2 \quad 3.4.9$$

The expression gives the rate of increase of mean concentration as a function of the local mean air concentration and the equilibrium air concentration appropriate to the local slope and may be used with the gradually varied flow equation in the next section to compute the air concentration down a spillway with a varying slope. For a spillway with a constant slope equation 3.4.8 alone is sufficient to compute the air concentrations down the spillway. However, the gradually varied flow equation is still necessary if velocities down the spillway are required.

3.4.3 The gradually varied flow equation in aerated flow on a steep chute with a variable bottom slope

The necessary equation is a simple extension of the normal gradually varied flow equation and is obtained by treating the aerated flow as if it were a continuous fluid with a varying density and velocity, Fig. 3.14. For this case the specific energy for a streamline at y above the bed is

$$E(y) = y \cos \theta + \frac{1}{\rho(y)g} \int_y^\infty \rho(y) g \cos \theta dy + \frac{(u(y))^2}{2g} \quad 3.4.10$$

* Aviemore data indicates a value of c_v of the order of about 5%.

The total specific energy flux is then

$$E_f = \int_0^{\infty} \rho(y) g E(y) u(y) dy \quad 3.4.11$$

and the mean specific energy is

$$\bar{SE} = E_f / \int_0^{\infty} \rho(y) u(y) g dy \quad 3.4.12$$

The density of the air water mixture is written as

$$\rho(y) = \rho[1 - c] \quad 3.4.13$$

This approximation is satisfactory for calculating the terms for potential and velocity energy in eqn 3.4.10 but the approximation of a hydrostatic pressure distribution in the outer regions of the flow is clearly not realistic. Fortunately downstream of the point of inception the hydrostatic pressure term is small and an acceptable approximation for the specific energy term is

$$\bar{SE} = d \cos\theta + \bar{E} \frac{u_w^2}{2g} \quad 3.4.14$$

where

$$\bar{E} = \left[\frac{u_{.9}}{u_w} \right]^{0.5} \frac{\int_0^{\infty} (1-c) u'^3 dy'}{\int_0^{\infty} (1-c) u' dy'} \quad 3.4.15$$

with $u' = u/u_{.9}$ and $y' = y/y_{.9}$. Measured values on Aviemore dam show that \bar{E} is independent of \bar{c} and has a value of 1.09. The elevation of the total energy line is then given by

$$H = d \cos\theta + \frac{1.09}{2g} \left(\frac{q}{d} \right)^2 + z \quad 3.4.16$$

where z is the vertical distance to the spillway floor from some datum.

Differentiating this equation with respect to x we obtain

$$\frac{dd}{dx} = \frac{\sin\theta - s_f + d \sin\theta \frac{d\theta}{dx}}{\cos\theta - 1.09 Fr^2} \quad 3.4.17^*$$

where $Fr^2 = q^2/gd^3$.

* This equation may also be modified to allow for a gradual variation in width (Appendix 3.2.4).

For a spillway with a constant slope equation 3.4.8. gives the air concentration as a function of x and this with Fig 3.10 yields s_f $[q^2 f_e / 8gd^3] \phi(\bar{c})$ and enables equation 3.4.17 to be integrated numerically.

For a spillway with a variable slope it is assumed that the slow growth of the aerated layer implies a local equilibrium and this suggests that Figure 3.10 can be used with local rather than equilibrium values. Equations 3.4.9 and 3.4.17 are two simultaneous ordinary differential equations and in conjunction with $\phi_2(c)$ (Fig. 3.10) and the value of c_e for each θ (Fig. 3.8) they can be solved using a simple numerical scheme. This reproduced the air entrainment on Aviemore spillway (Fig. 3.15, a and b).

Indeed these equations provide a method of computing all the flow properties including the air concentration close to the bed downstream of the start of air entrainment for spillways.

3.5 CONCLUSION

This chapter gives the equations which enable estimates of the depths up to the point of inception (3.2) and depths, mean air concentrations and air concentration distributions downstream of the point of inception (3.4) for any spillway chute. The methods of solution are suggested and it is relatively straight forward to write a program to solve these equations.

The calculations to the point of inception depend on boundary layer theory and an interpretation of the numerical work of Keller & Rastogi [1977]. Downstream of the point of inception they depend on Straub and Anderson's [1958] classic laboratory measurements [for the equilibrium air concentration and the variation of friction factor with mean air concentration] and Cains [1978] Aviemore spillway measurement [for the velocity distribution in the aerated flow and for an equation for the rate of air entrainment]. These sets of measurements are consistent but to obtain an independent check there is a need for further prototype measurements.

3.5 LIST OF SYMBOLS

a	[m]	a typical spillway dimension
b	[m]	the spillway width
c	[-]	the air concentration [volume of air]/[volume of air + volume of water]
\bar{c}	[-]	the depth averaged air concentration
$\bar{c}(x)$	[-]	the local depth averaged air concentration
c_b	[]	the air concentration at the spillway surface
\bar{c}_e	[-]	the depth averaged equilibrium air concentration
c_v	[-]	the air concentration due to longitudinal vortices
d	[m]	the equivalent clear water depth
d_{cs}	[m]	a length scale $(q^2/g \sin\theta)^{0.33}$
d_e	[m]	the equivalent clear water depth at the equilibrium air concentration $[\bar{c}_e]$
d_I	[m]	the water depth at the point of inception of air entrainment
$E(y)$	[m]	the specific energy on a streamline a distance y above the spillway surface
E_f	[m]	the flux the specific energy
E'	[m]	a kinetic energy correction factor
f	[-]	the friction factor for clear water
f_c	[-]	the friction factor for water with a depth averaged air concentration of c
f_e	[-]	the friction factor at the equilibrium air concentration
$Fr(x)$	[-]	the local Froude number at x
g	[m/s ²]	the acceleration of gravity
h	[m]	the head above the dam crest
h_s	[m]	the vertical distance from the spillway surface to the elevation of the water in the dam
H	[m]	the elevation above a datum of the Total Energy line

k_s	[m]	the equivalent sand roughness of the spillway surface
n	[-]	the constant in the power law approximation for the boundary layer velocity distribution
q	[m ² /s]	the water discharge for a unit width of spillway
q_a	[m ² /s]	the air discharge for a unit width of spillway
q_δ	[m ² /s]	the water discharge per unit width within the boundary layer
$q_{1.2\delta}$	[m ² /s]	the discharge/unit width between 1.2 times the boundary layer thickness and the spillway surface
Q	[m ³ /s]	the total spillway discharge
Q_δ	[m ³ /s]	the total discharge within the boundary layer
r	[-]	a correlation coefficient
S	[-]	the spillway slope
S_f	[-]	the friction slope
\overline{SE}	[m]	the mean specific energy
u	[m/s]	the water velocity
u_a	[m/s]	the air velocity
u_{fs}	[m/s]	the free streamline velocity
u_w	[m/s]	the depth averaged water velocity
u_I	[m/s]	the free surface velocity at the point of inception
u_m	[m/s]	the mixture velocity
$u_{.9}$	[m]	the velocity where the air concentration is 90%
u'	[]	$u/u_{.9}$
v_e	[m/s]	an entrainment velocity
v_w	[m/s]	the fall velocity of water droplets in air
x	[m]	a distance measured along the spillway surface
x_I	[m]	the mean distance from the start of the growth of the boundary layer to where it reaches the free surface
x_s	[m]	a boundary slope distance [Fig. 3.2]
y	[m]	a distance measured perpendicular to the spillway surface

$y_{.9}$	[m]	the distance from the spillway surface to where the air concentration is 90%
y'	[]	$y/y_{.9}$
z	[m]	the vertical distance from a datum to the spillway surface
α	[-]	a constant in the boundary layer growth equation
β	[-]	a constant in the boundary layer growth equation
β_e	[-]	the equilibrium entrainment constant
$\beta(x)$	[-]	the local entrainment constant
γ	[N/m ³]	the specific weight
δ	[m]	the boundary layer thickness
ϵ	[1/s]	the diffusivity of the average density in an air/water mixture
ϕ	[-]	a function
θ	[°]	the spillway slope
ρ	[Kg/m ³]	the density
ρ_a	[Kg/m ³]	the air density
ρ_w	[Kg/m ³]	the water density
ν	[m ² /s]	the kinematic viscosity



Fig. 3.1 Self-aerated flow on the spillway of Aviemore Dam, Waitaki River, New Zealand. The spillway gates are open 600 mm except for the middle gate where the opening is 300 mm.

Note (1) the change from clear water to white water. This change marks the point of inception of air entrainment.

Note (2) the longitudinal vortices in the clear water above the point of inception. These are thought to be caused by the stretching of the vorticity that is established in the reservoir.

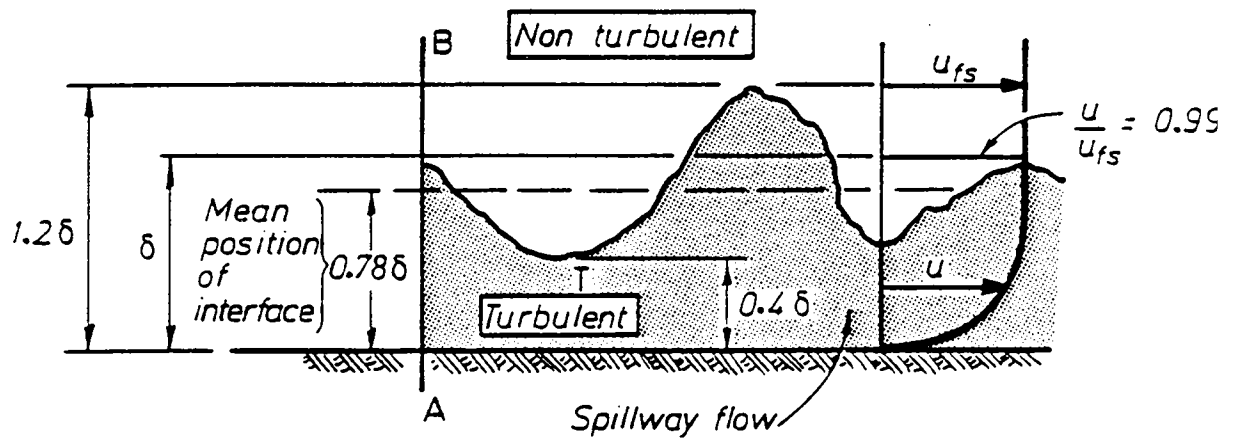
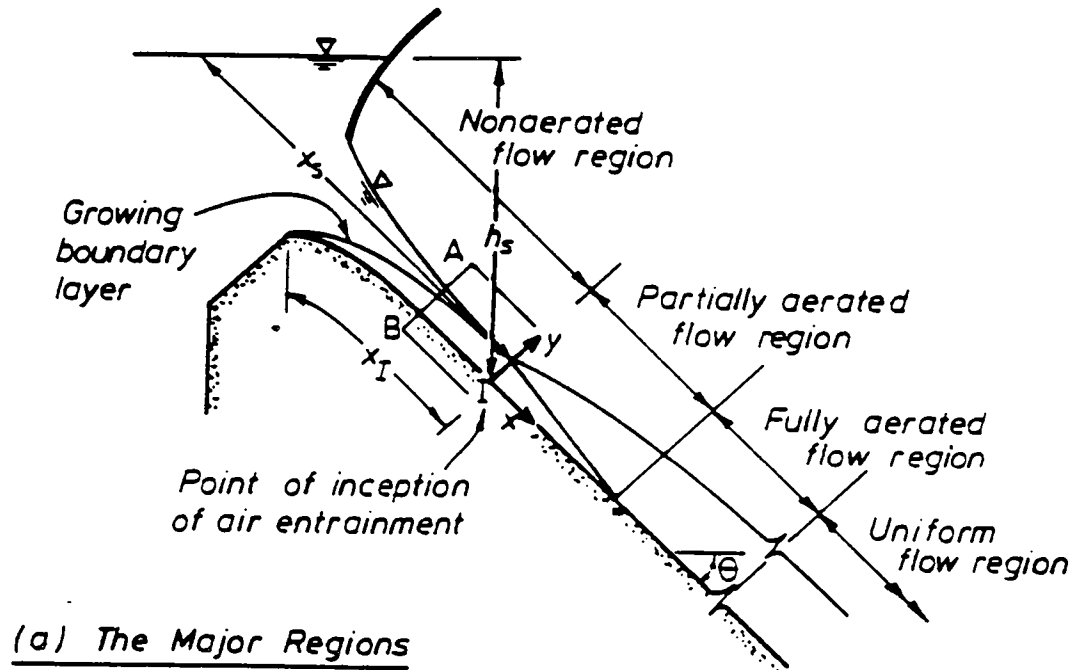


Fig. 3.2 The regions in a self-aerated flow down a spillway

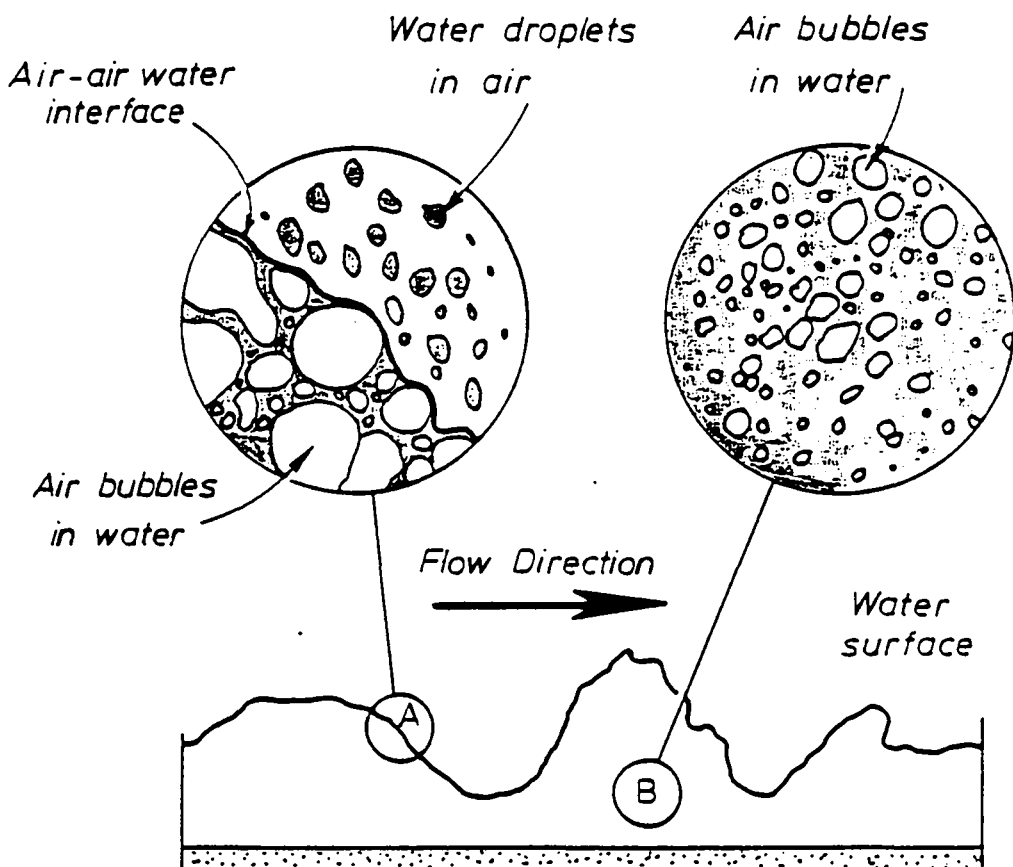


Fig. 3.3 The detailed structure in the region of fully aerated flow

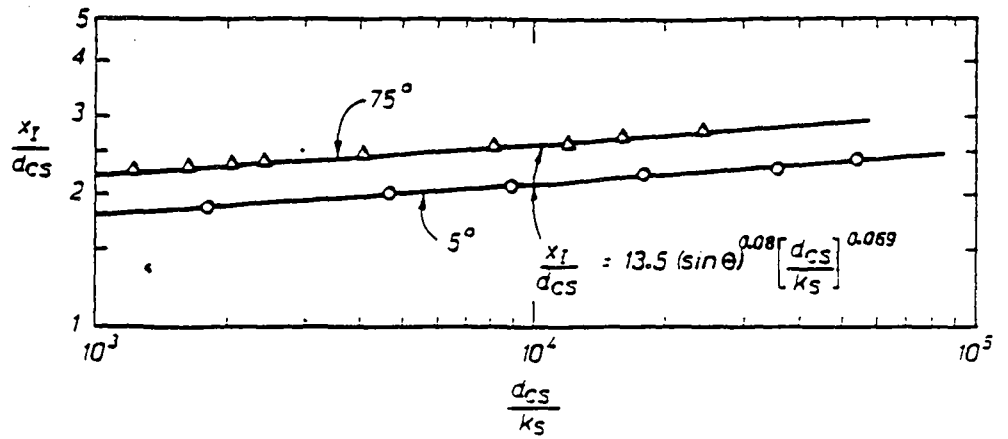


Fig. 3.4 The position on a standard spillway where the computed boundary layer defined by $u/u_{fs} = 0.99$ reaches the free surface. The plotted points are those from Keller & Rastogi 1977. The other properties at this point are given by

$$\frac{u_I}{(2g d_{cs})^{0.5}} = 3.68 [\sin \theta]^{0.54} \left[\frac{d_{cs}}{k_s} \right]^{0.035}$$

$$\frac{d_I}{d_{cs}} = \frac{0.22}{[\sin \theta]^{0.04}} \left[\frac{d_{cs}}{k_s} \right]^{-0.035}$$

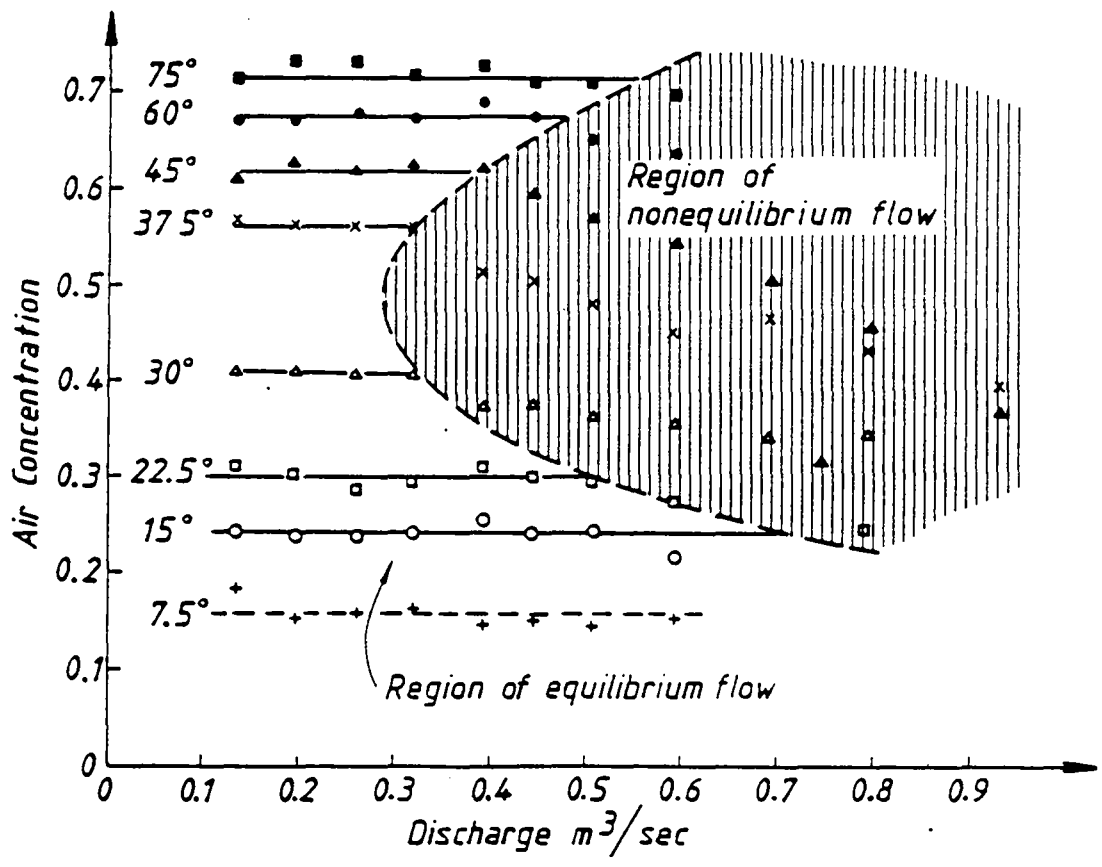


Fig. 3.5 The mean air concentration plotted against discharge for Straub and Anderson's results

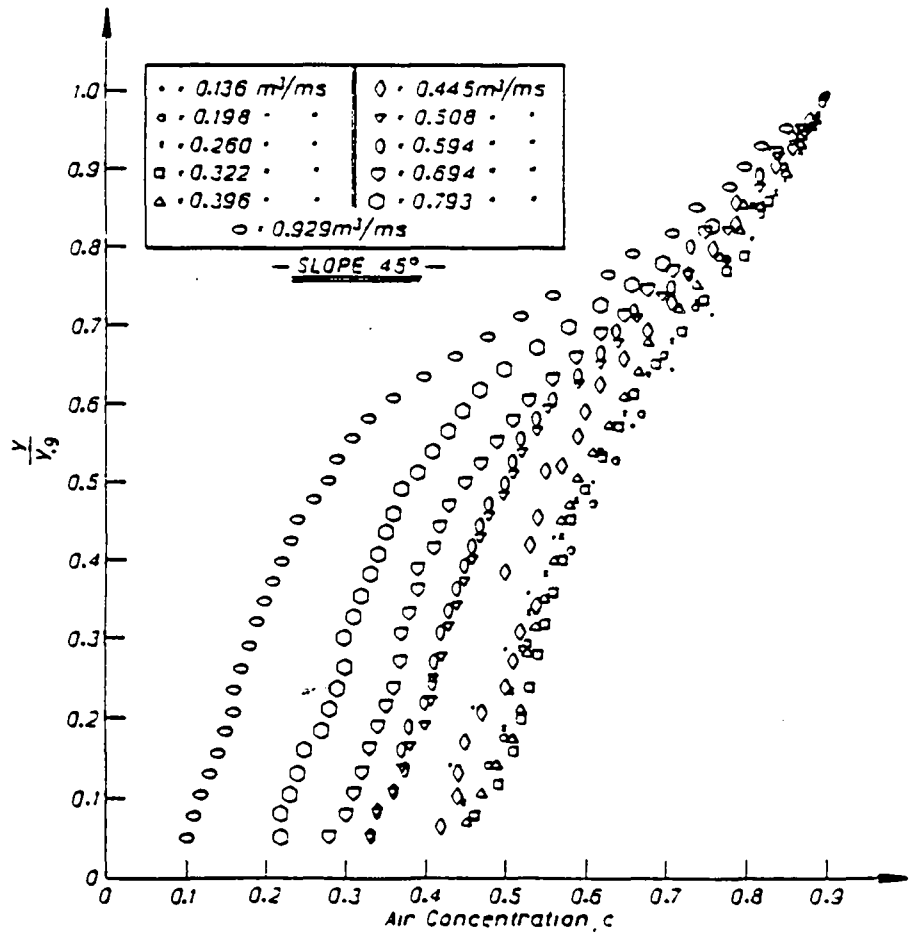


Fig. 3.6 Straub and Anderson's measurements of air concentrations in the "uniform" flow region for a slope of 45°

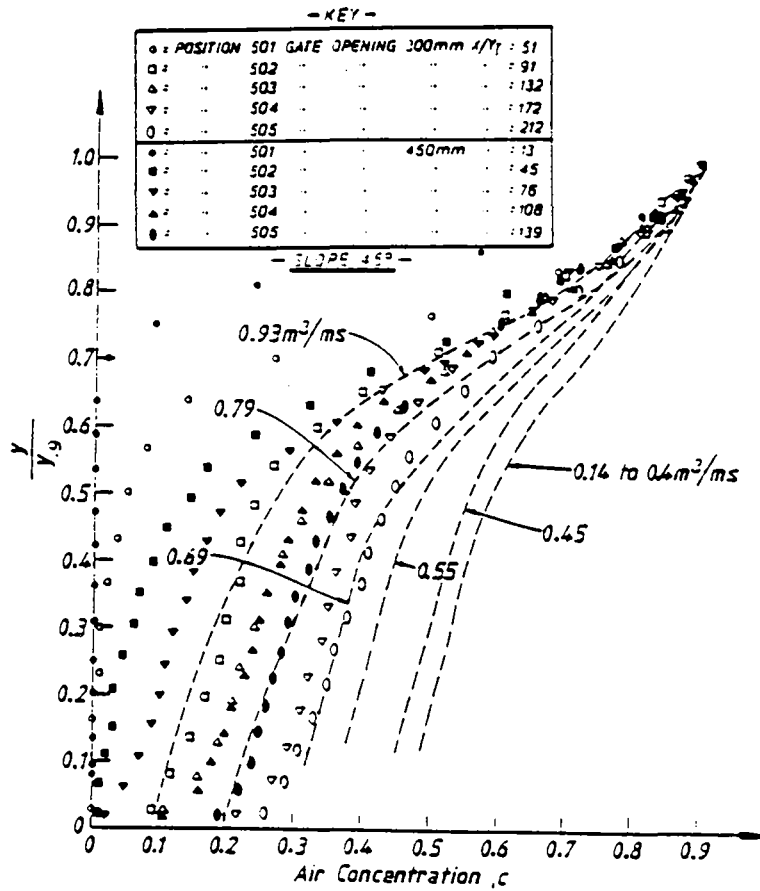


Fig. 3.7 Straub and Anderson's measurements of air concentration in the "uniform" flow region compared with those in the developing region made by Cain (1978)

The dashed lines are those obtained from Straub and Anderson's results.

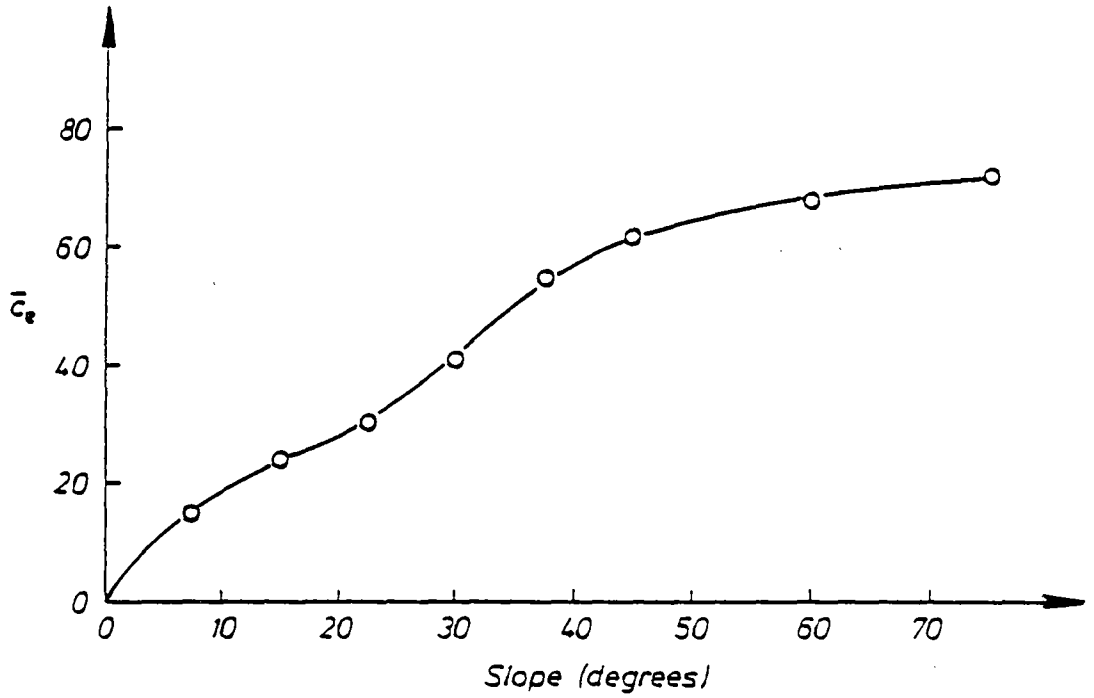


Fig. 3.8 The equilibrium mean air concentration defined as a function of slope

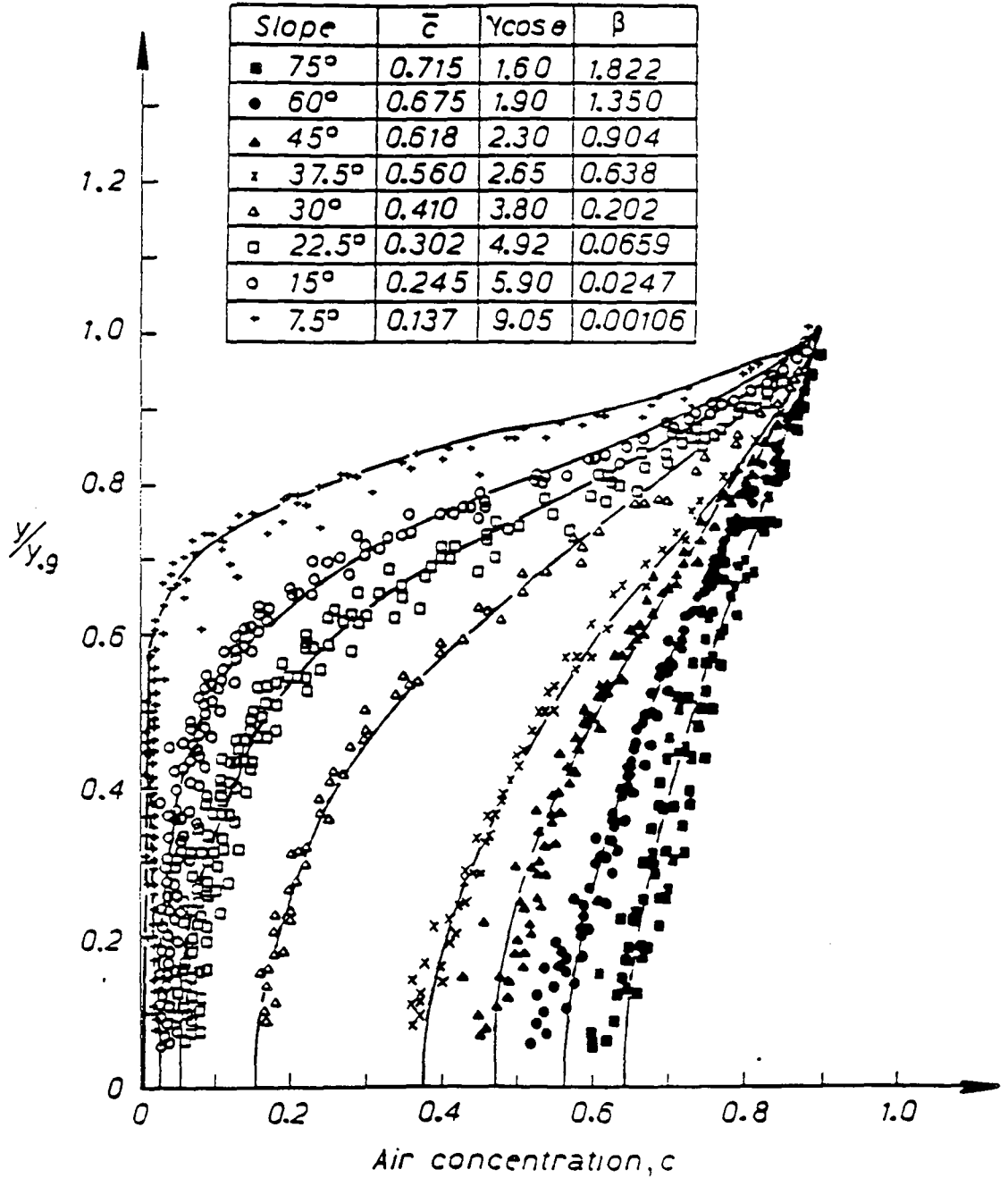


Fig. 3.9 A comparison of the air concentration distribution from the analytic theory with Straub and Anderson's (1958) measurements

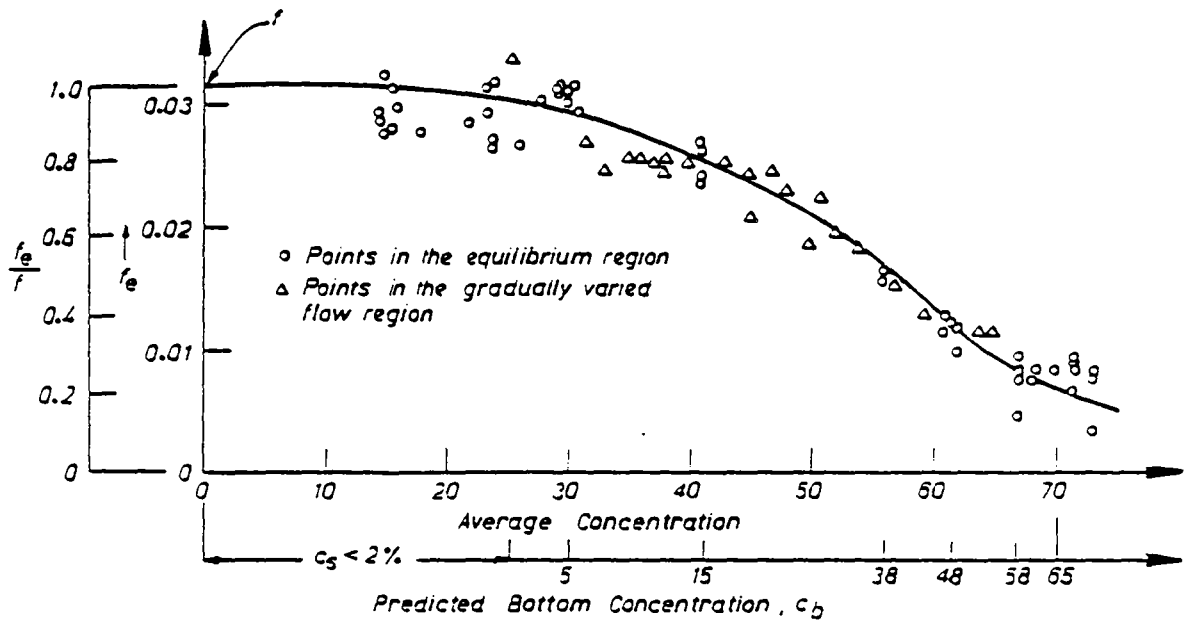


Fig. 3.10 The equilibrium friction factor f_e computed from Straub and Anderson's results as a function of the air concentration. Also included in this figure is the scale f_e/f and the calculated concentration of the spillway floor. This latter must be regarded as very approximate. Indeed Chanson's (1988) measurements and his examination of Cain's 1978 data suggest that these values are high.

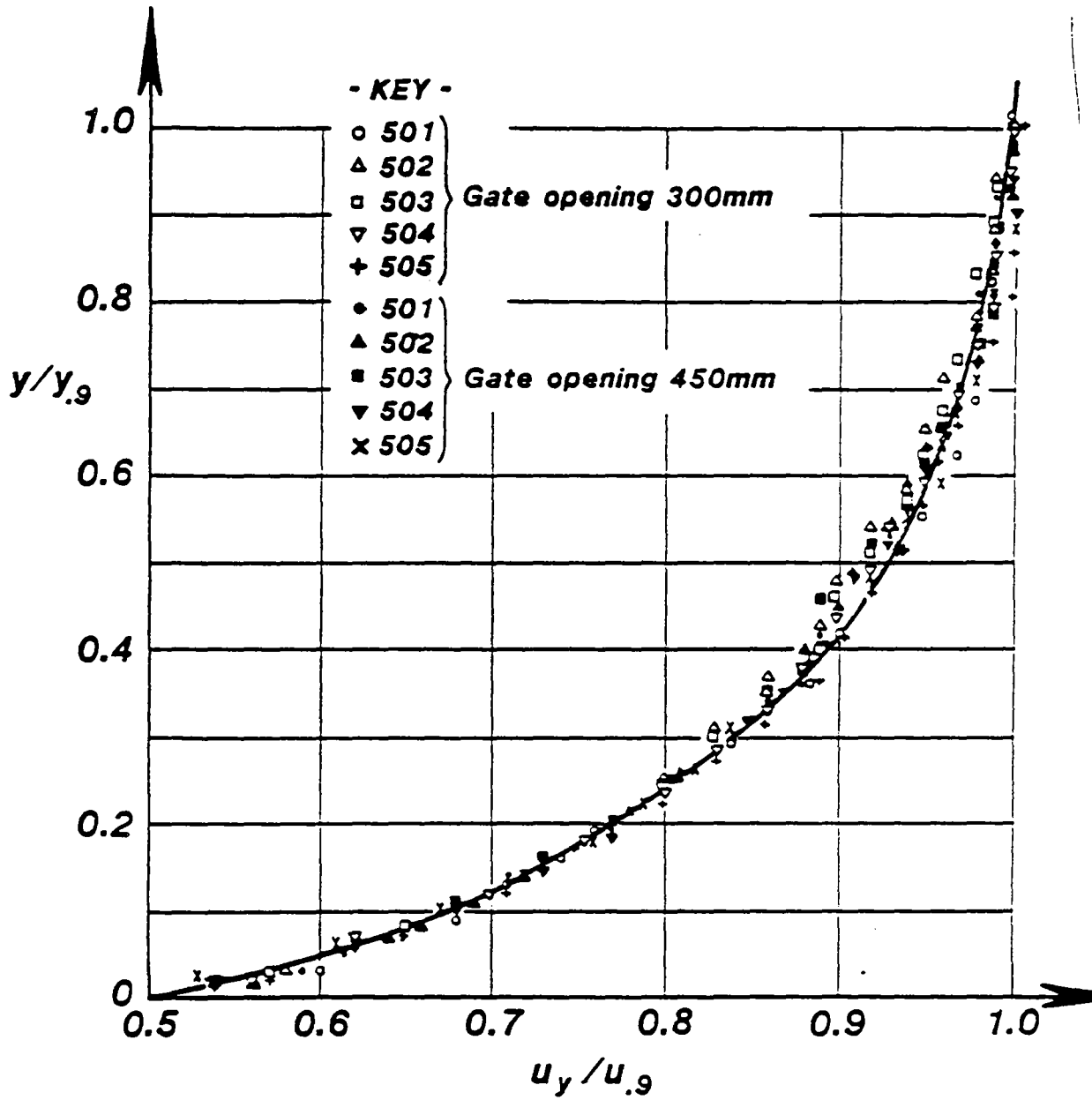


Fig. 3.11 The non-dimensional velocity distribution. These data are from Cain's Aviemore measurements and is for an average air concentration (Equation 3.3.3) ranging from 5 to 50%.

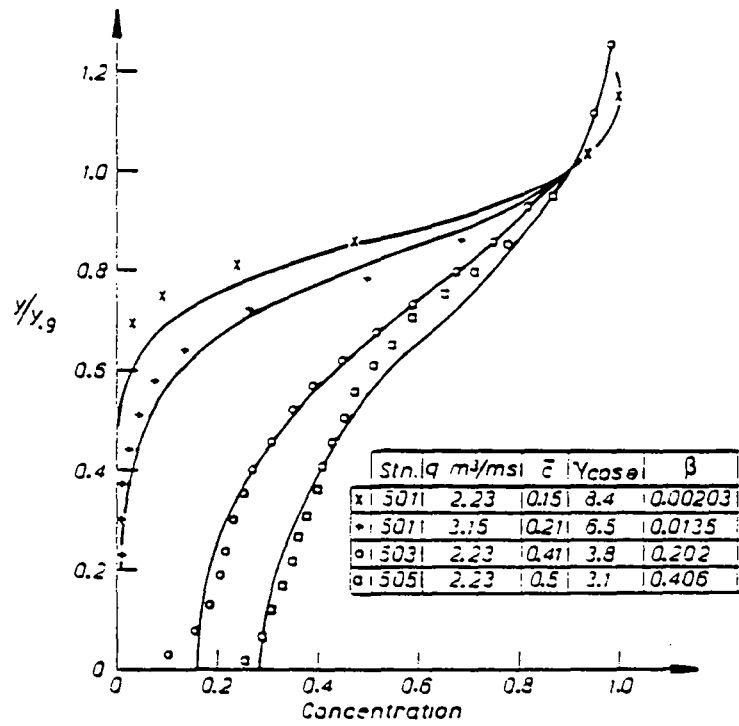


Fig. 3.12 A comparison of Cain's measured air concentrations and the computed equilibrium air concentrations

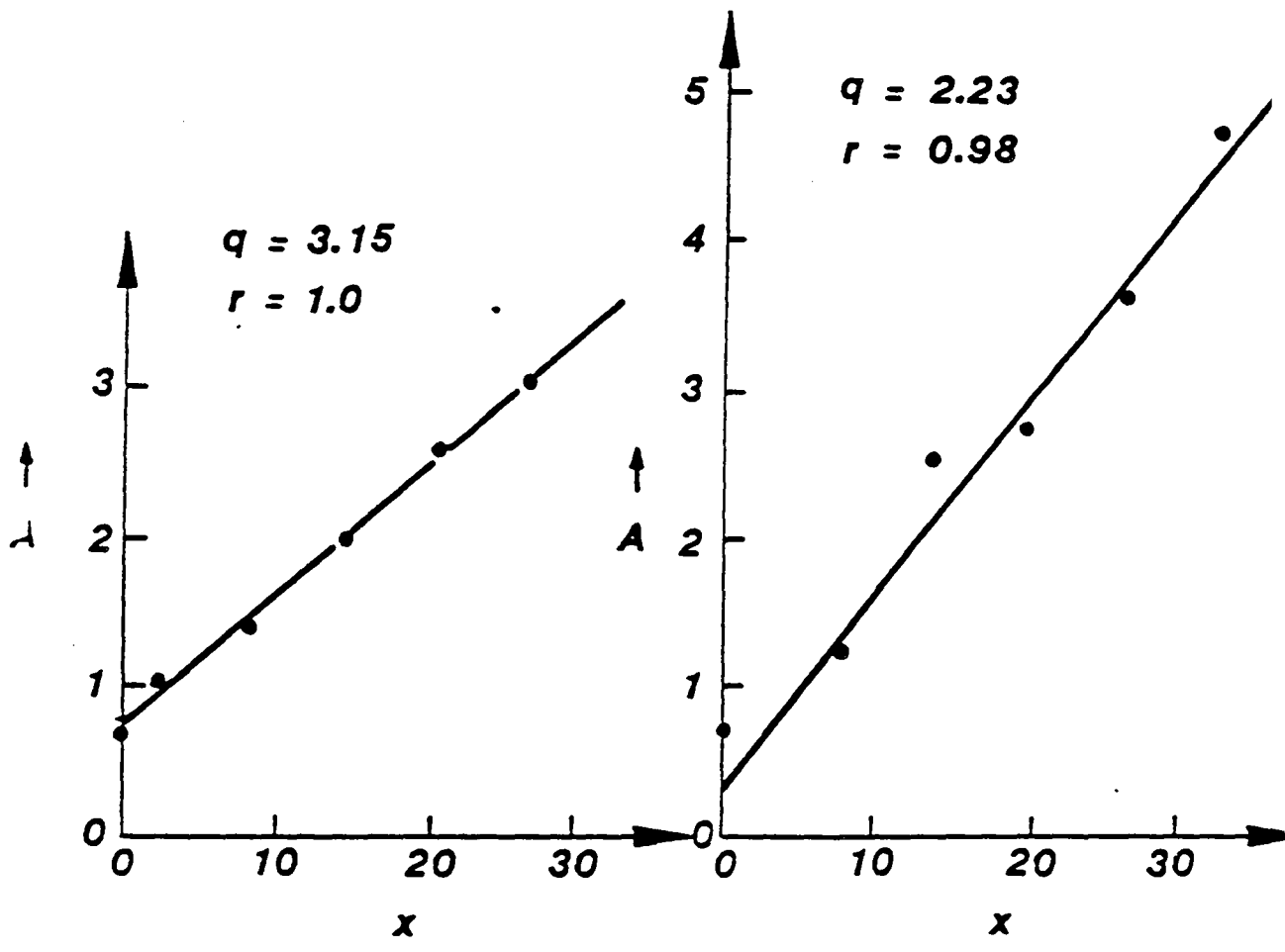


Fig. 3.13 The form of the entrainment function.

A is the left hand side of equation 3.4.8.

i.e.

$$A = \frac{1}{(1 - \bar{c}_e)^2} \ln \frac{(1 - \bar{c}(x))}{(\bar{c}_e - \bar{c}(x))} - \frac{1}{(1 - \bar{c}_e)(1 - \bar{c}(x))}$$

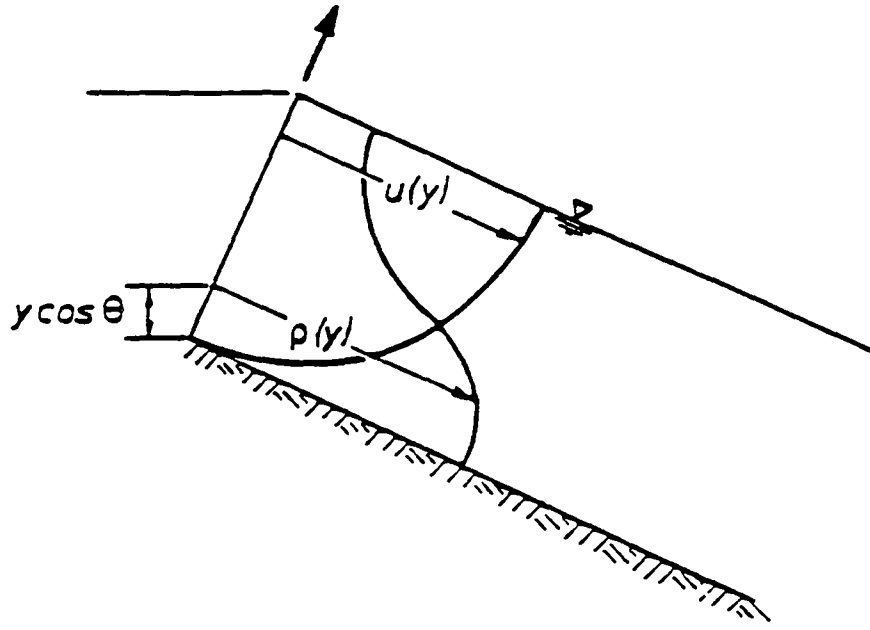


Fig. 3.14 A free surface flow with a varying density and velocity

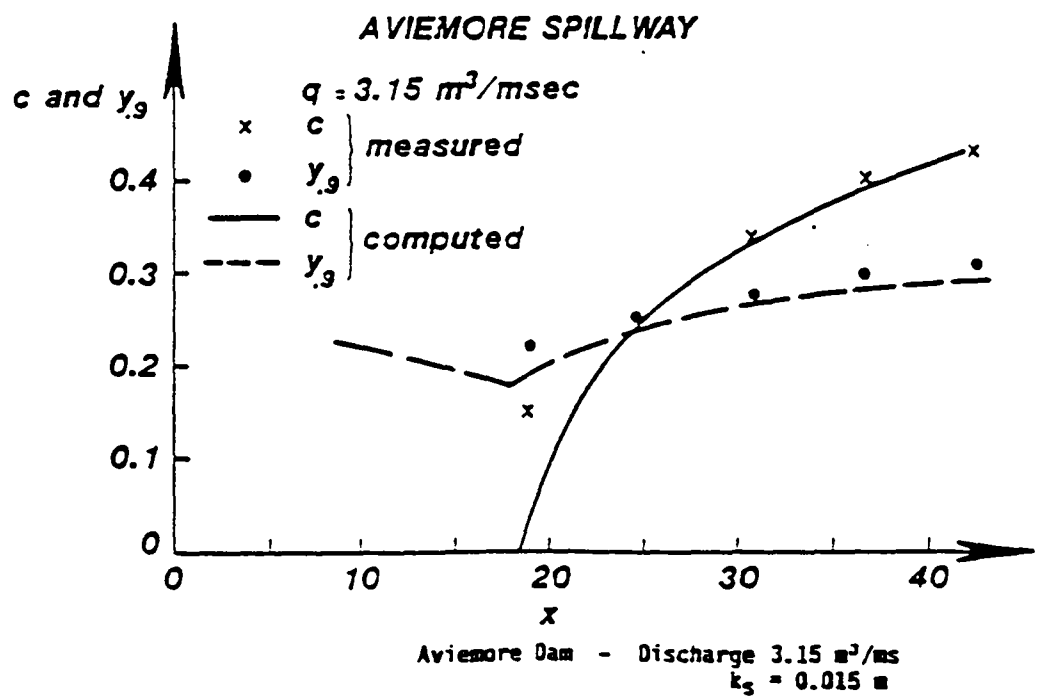
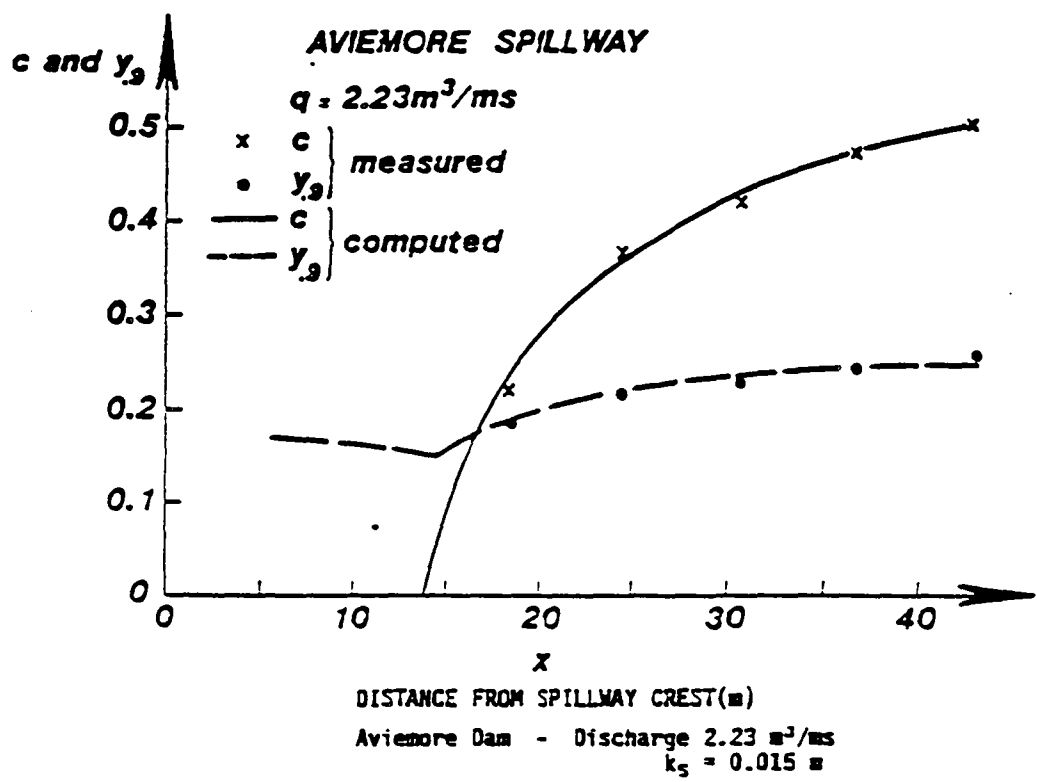


Fig. 3.15 A check on the consistency of the solutions of equations 3.4.9 and 3.4.17. A comparison of measured (Cain 1978) and computed data for Aviemore Spillway

Appendix 3.1 The Calculation of the Rate of Boundary Layer
Growth on Spillways with Slowly Varying Slope and Width

The boundary layer thickness for a standard spillway equation 3.2.0 can be written as

$$\frac{\delta}{x} = 0.0212[\sin\theta]^{-0.11} \left(\frac{x}{k_s} \right)^{-0.1} \quad 3.1.1$$

Differentiating this equation yields

$$\frac{d\delta}{dx} = \frac{\delta}{x} \left(0.9 - 0.11 \cot\theta \times \frac{d\theta}{dx} \right) \quad 3.1.2$$

Assuming the velocity distribution in the boundary layer is given by

$$\frac{u}{u_{fs}} = \left(\frac{y}{y_{0.9}} \right)^{1/n} \quad 3.1.3$$

then the flow within the boundary layer is approximately

$$q_\delta = \frac{n\delta}{n+1} \sqrt{2gh_s}$$

and

$$\frac{dq_\delta}{dx} = v_e = q_\delta \left(\frac{1}{2} \frac{\sin\theta}{h_s} + \frac{1}{\delta} \frac{d\theta}{dx} \right) \quad 3.1.4$$

$$v_e = q_\delta \left(\frac{1}{2} \frac{\sin\theta}{h_s} + \frac{0.9}{x} - 0.11\cot(\theta) \frac{d\theta}{dx} \right) \quad 3.1.5$$

This is the velocity of entrainment into the boundary layer on a standard spillway.

Now for a spillway channel with slightly diverging or converging walls

$$Q_\delta = \frac{wn\delta}{(n+1)} \sqrt{2gh_s} \quad 3.1.6$$

Where Q_δ is the total discharge with the boundary layer and w is the spillway width

$$\frac{dQ_\delta}{dx} = \frac{n}{n+1} v \sqrt{2gh_s} \cdot \delta \left(\frac{1}{v} \frac{dv}{dx} + \frac{\sin\theta}{2H_s} + \frac{1}{\delta} \frac{d\delta}{dx} \right) \quad 3.1.7$$

and

$$\frac{1}{v} \frac{dQ_\delta}{dx} = v_e = q_\delta \left(\frac{1}{\delta} \frac{dv}{dx} + \frac{\sin\theta}{2h_s} + \frac{1}{\delta} \frac{d\delta}{dx} \right) \quad 3.1.8$$

If the changes in θ and the width changes are sufficiently small then the entrainment velocity obtained from the standard spillway calculations is applicable. Thus substituting from equation 3.1.4 into equation 3.1.8 we obtain

$$\frac{d\delta}{dx} = \delta \left(\frac{0.9}{x} - 0.11 \cot\theta \frac{d\theta}{dx} - \frac{1}{v} \frac{dv}{dx} \right) \quad 3.1.9$$

or

$$\frac{d\delta}{dx} = \frac{\delta}{x} \left(0.9 - 0.11 \cot\theta \frac{d\theta}{dx} - \frac{x}{v} \frac{dv}{dx} \right) \quad 3.1.10$$

Appendix 3/2

For comparison Measurement

Appendix 3.2 Air Concentration Measurements

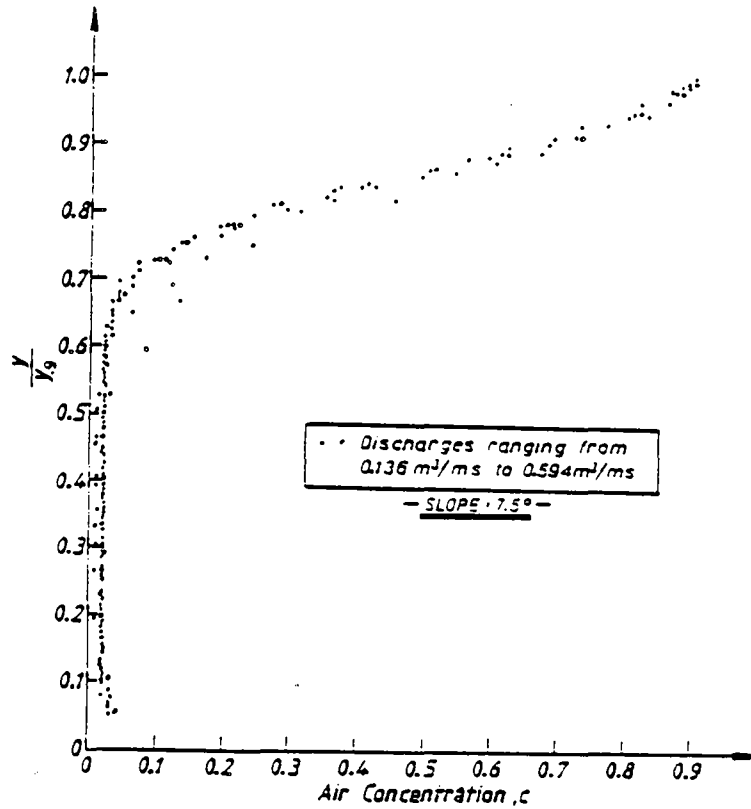


Fig. 3.2.1 Measurements of air concentration for a 7.5° slope

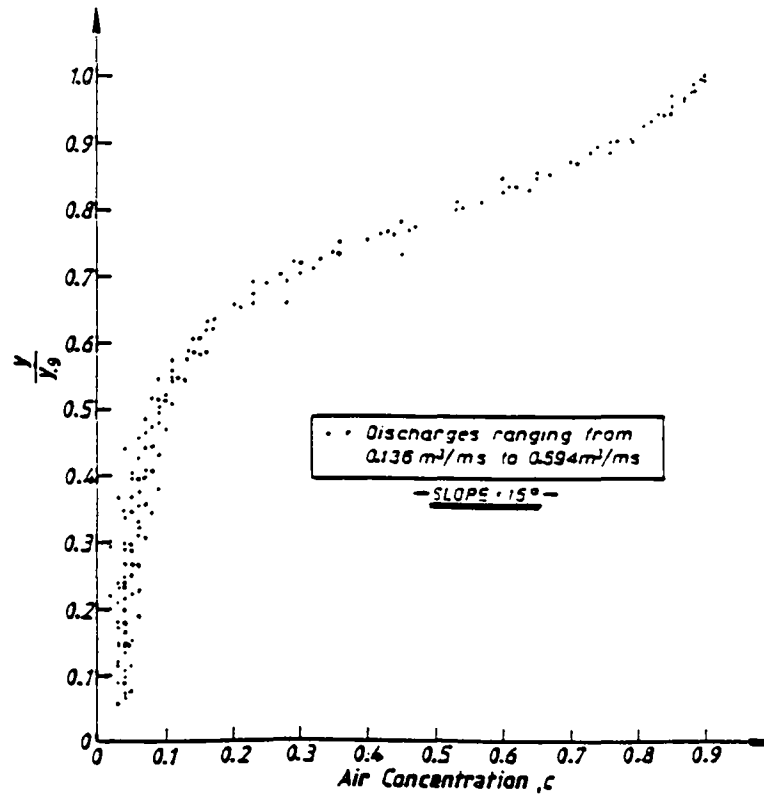


Fig. 3.2.2 Measurements of air concentration for a 15° slope

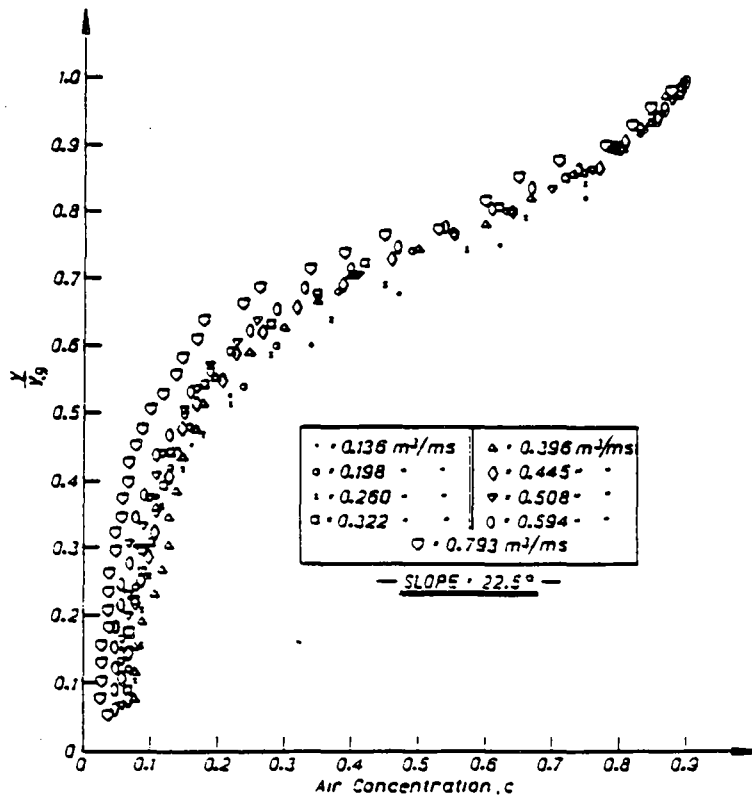


Fig. 3.2.3 Measurements of air concentration for a 22.5 slope

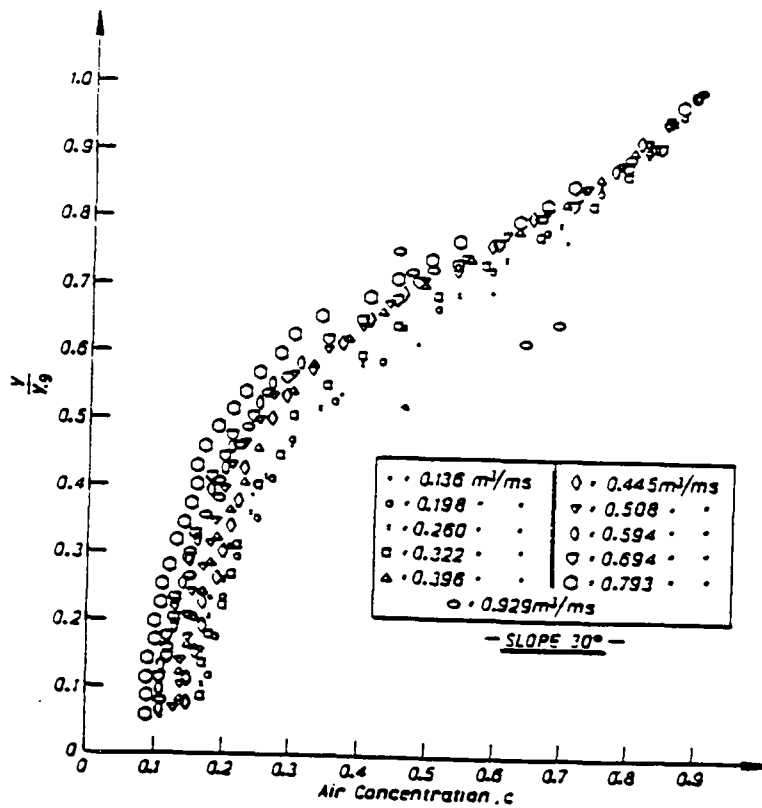


Fig. 3.2.4 Measurements of air concentration for a 30° slope

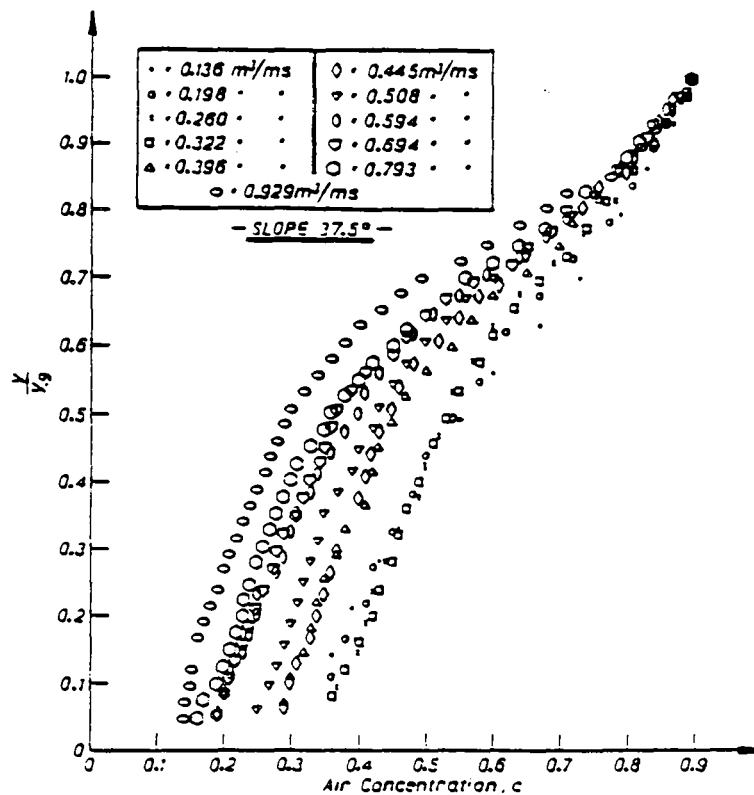


Fig. 3.2.5 Measurements of air concentration for a 37.5° slope

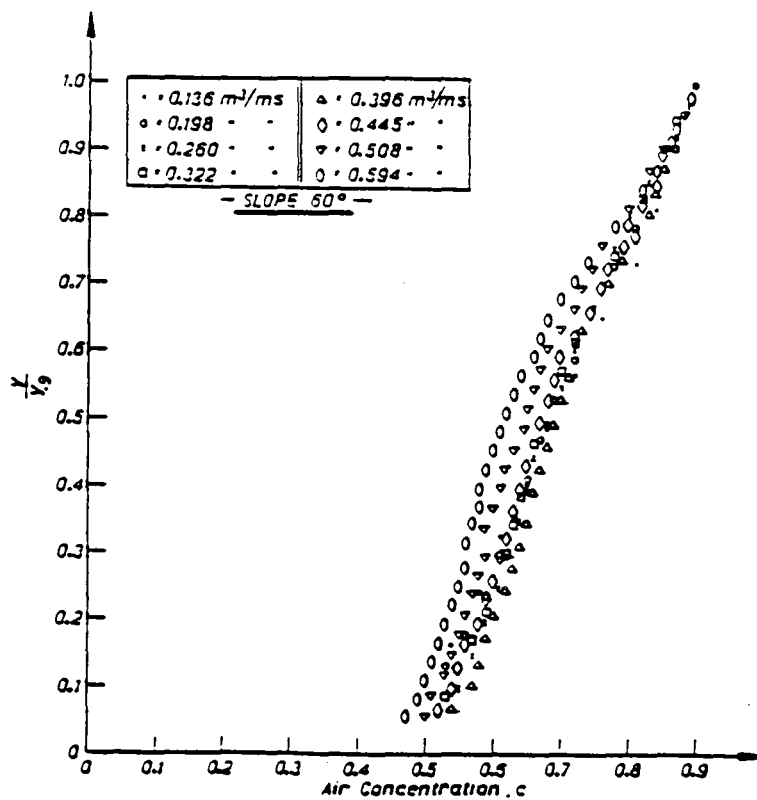


Fig. 3.2.6 Measurements of air concentration for a 60° slope

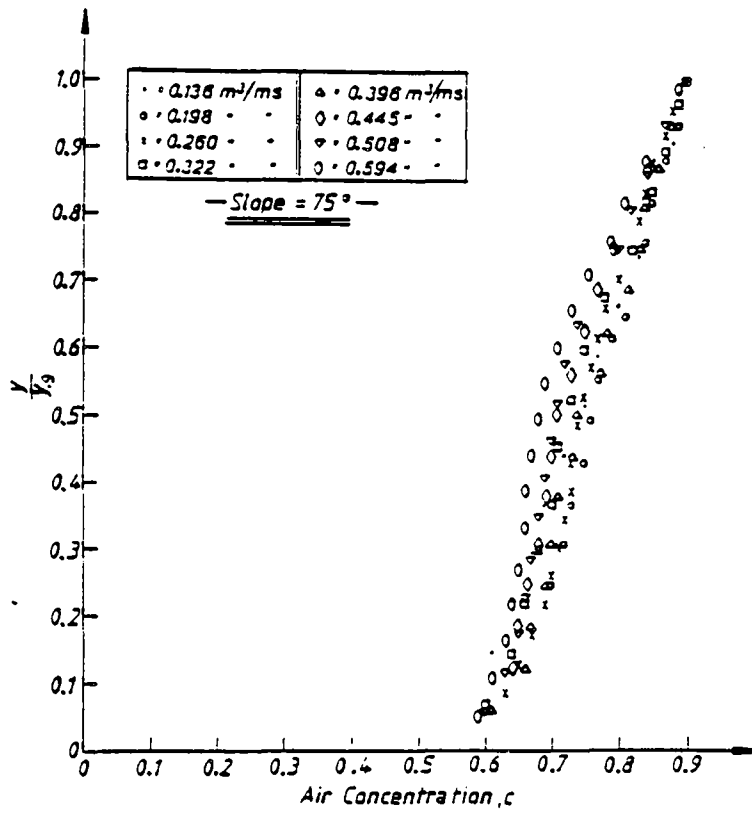


Fig. 3.2.7 Measurements of air concentration for a 75° slope

Appendix 3.3

The Equilibrium Air Concentration Distributions

The conservation equation for the mixture density in the equilibrium region where everything is independent of x is

$$\epsilon \frac{d}{dy} [\rho(1-c)] = \rho(1-c)v_w \cos\theta \quad 3.3.1$$

where ϵ is the diffusivity of the average density and since $\rho(1-c)$ is in effect the mass of water per unit volume, v_w is to be associated with the fall velocity of the water. When c is large we have water droplets in air and v_w should be the fall velocity of water droplets in air. However when c is small we have the situation of a few air bubbles rising through water and thus the downward velocity of the water is small. Finally at the solid surface we have $v_w = 0$. An assumption which may be used to satisfy these conditions between $y = 0$ and $y = y_0$ (but not outside this range) is

$$v_w \propto cy \quad 3.3.2$$

Without prior knowledge of the air concentration distribution it is not possible to make reasonable assumptions about ϵ so the simplest assumption of a constant ϵ will be used. Substituting into equation 3.3.1 and integrating yields

$$c = \frac{\beta}{\beta + e^{\gamma \cos\theta y'^2}} \quad 3.3.3$$

where y' is the non-dimensional depth and where β and γ are constants. The condition that $c = 0.9$ when $y' = 1$ yields one relationship between the constants $(0.9 = \beta / (\beta + e^{\gamma \cos\theta}))$ and the second relationship is from the desired mean air concentration (Fig. 3.1).

5%

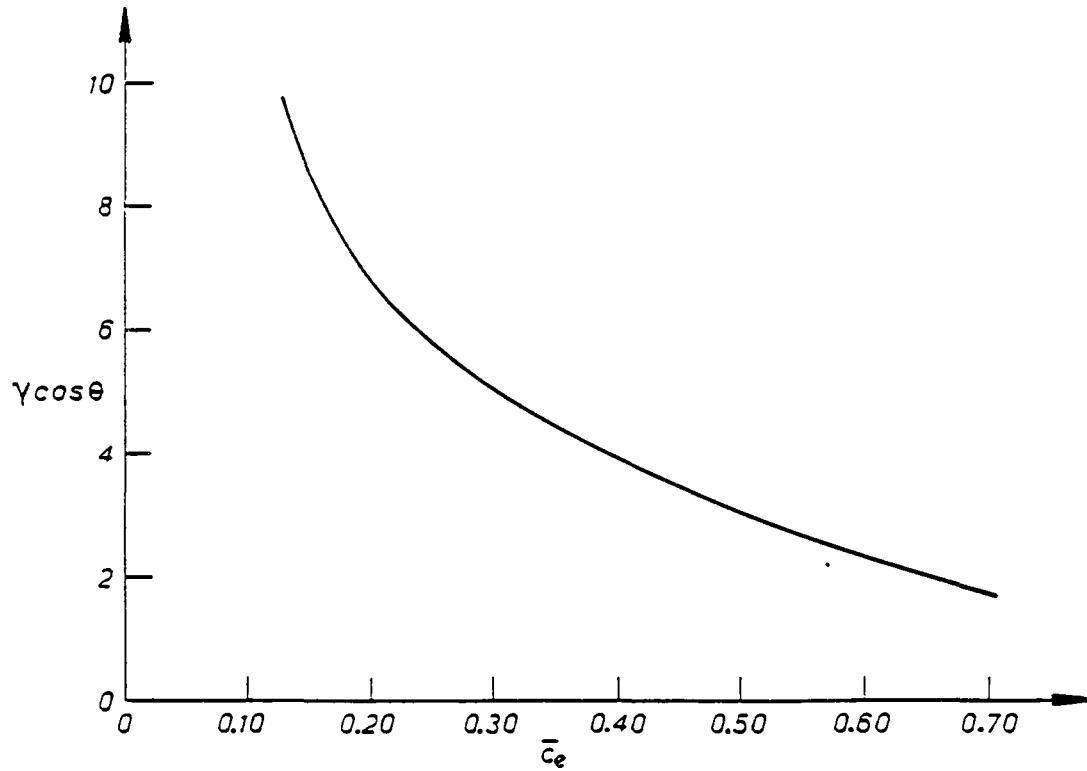


Figure 3.3.1 A plot of $\gamma \cos \theta$ vs. the equilibrium air concentration \bar{c}_e

Appendix 3.4 The Gradually Varied Flow Equation
on a Steep Slope With Slowly Varying Slope and Width

The elevation of the total energy line above a section on the spillway is given by

$$H = z + d \cos \theta + \frac{\bar{E}}{2g} \left(\frac{Q}{bd} \right)^2$$

where z = height above some datum

Q = total discharge

b = width

\bar{E} = an energy correction factor which for the Aviemore data was almost independent of \bar{c} and had a value of 1.05.

Differentiating

$$\frac{dH}{dx} + \frac{dz}{dx} + \frac{dd}{dx} \cos \theta - d \sin \theta \frac{d\theta}{dx} - \frac{1.09}{g} \left(\frac{Q}{bd} \right)^2 \frac{1}{d} \frac{dd}{dx} - \frac{1.09}{g} \left(\frac{Q}{bd} \right)^2 \frac{1}{b} \frac{db}{dx} = 0$$

or noting that

$$\frac{dH}{dx} = S_f$$

and $\frac{dz}{dx} = -\sin \theta$ and $q = Q/b$

we get

$$\frac{dd}{dx} = \frac{\sin \theta \left(1 + d \frac{d\theta}{dx} \right) + 1.09 \frac{q^2}{gd^2} \frac{1}{b} \frac{db}{dx} - S_f}{\cos \theta - \frac{1.09}{g} \frac{q^2}{d^3}}$$

Multiplying the top and bottom by d^3 , making use of the fact that the flow is gradually varied such that the local friction factor (f_c) will have the same value as the friction factor with the same average concentration (f_e) and noting that

$$d^3 S_f = \frac{q^2 f_c}{2Ag} = \frac{q^2}{Ag} f \left(\frac{f_e}{f} \right) = A \left(\frac{f_e}{f} \right)$$

where $A = \frac{q^2 f}{Ag}$

Then
$$\frac{dd}{dx} = \frac{d^3 \sin\theta \left(1 + d \frac{d\theta}{dx}\right) + 1.09 B \cdot d \cdot \frac{db}{dx} / b - A \left(\frac{f_e}{f}\right)}{d^3 \cos\theta - 1.09 B}$$

where $B = q^2/g$

3.5 LIST OF SYMBOLS

a	[m]	a typical spillway dimension
b	[m]	the spillway width
c	[-]	the air concentration [volume of air]/[volume of air + volume of water]
\bar{c}	[-]	the depth averaged air concentration
$\bar{c}(x)$	[-]	the local depth averaged air concentration
c_b	[]	the air concentration at the spillway surface
\bar{c}_e	[-]	the depth averaged equilibrium air concentration
c_v	[-]	the air concentration due to longitudinal vortices
d	[m]	the equivalent clear water depth
d_{cs}	[m]	a length scale $(q^2/g \sin\theta)^{0.33}$
d_e	[m]	the equivalent clear water depth at the equilibrium air concentration $[\bar{c}_e]$
d_I	[m]	the water depth at the point of inception of air entrainment
$E(y)$	[m]	the specific energy on a streamline a distance y above the spillway surface
E_f	[m]	the flux the specific energy
E'	[m]	a kinetic energy correction factor
f	[-]	the friction factor for clear water
f_c	[-]	the friction factor for water with a depth averaged air concentration of c
f_e	[-]	the friction factor at the equilibrium air concentration
$Fr(x)$	[-]	the local Froude number at x
g	[m/s ²]	the acceleration of gravity
h	[m]	the head above the dam crest
h_s	[m]	the vertical distance from the spillway surface to the elevation of the water in the dam
H	[m]	the elevation above a datum of the Total Energy line

k_s	[m]	the equivalent sand roughness of the spillway surface
n	[-]	the constant in the power law approximation for the boundary layer velocity distribution
q	[m ² /s]	the water discharge for a unit width of spillway
q_a	[m ² /s]	the air discharge for a unit width of spillway
q_δ	[m ² /s]	the water discharge per unit width within the boundary layer
$q_{1.2\delta}$	[m ² /s]	the discharge/unit width between 1.2 times the boundary layer thickness and the spillway surface
Q	[m ³ /s]	the total spillway discharge
Q_δ	[m ³ /s]	the total discharge within the boundary layer
r	[-]	a correlation coefficient
S	[-]	the spillway slope
S_f	[-]	the friction slope
\overline{SE}	[m]	the mean specific energy
u	[m/s]	the water velocity
u_a	[m/s]	the air velocity
u_{fs}	[m/s]	the free streamline velocity
u_w	[m/s]	the depth averaged water velocity
u_I	[m/s]	the free surface velocity at the point of inception
u_m	[m/s]	the mixture velocity
$u_{.9}$	[m]	the velocity where the air concentration is 90%
u'	[]	$u/u_{.9}$
V_e	[m/s]	an entrainment velocity
V_w	[m/s]	the fall velocity of water droplets in air
x	[m]	a distance measured along the spillway surface
x_I	[m]	the mean distance from the start of the growth of the boundary layer to where it reaches the free surface
x_s	[m]	a boundary slope distance [Fig. 3.2]
y	[m]	a distance measured perpendicular to the spillway surface

$y_{.9}$	[m]	the distance from the spillway surface to where the air concentration is 90%
y'	[]	$y/y_{.9}$
z	[m]	the vertical distance from a datum to the spillway surface
α	[-]	a constant in the boundary layer growth equation
β	[-]	a constant in the boundary layer growth equation
β_e	[-]	the equilibrium entrainment constant
$\beta(x)$	[-]	the local entrainment constant
γ	[N/m ³]	the specific weight
δ	[m]	the boundary layer thickness
ϵ	[1/s]	the diffusivity of the average density in an air/water mixture
ϕ	[-]	a function
θ	[°]	the spillway slope
ρ	[Kg/m ³]	the density
ρ_a	[Kg/m ³]	the air density
ρ_w	[Kg/m ³]	the water density
ν	[m ² /s]	the kinematic viscosity

THE AIR DEMAND DATA AND PLANS OF SOME PROTOTYPE AERATORS

FOZ DO AREIA

Q	q	h	V	F _r	c/h	D/h**	Q _{ar}	q _{ar}	B	B _e ***
AERATOR No. 1										
1470	20.82	0.81	25.71	9.12	0.247	0.19	666	9.43	0.45	0.41
1000	14.16	0.59	24.01	9.98	0.339	0.26	554	7.85	0.55	0.52
850	12.04	0.52	23.15	10.25	0.385	0.30	515	7.29	0.61	0.57
690	9.77	0.46	21.25	10.00	0.435	0.34	453	6.42	0.66	0.61
535	7.58	0.38	19.94	10.33	0.526	0.41	395	5.59	0.74	0.69
2090	29.60	1.08	27.41	8.42	0.185	0.14	732	10.37	0.35	0.32
3300	46.74	1.64	28.50	7.11	0.122	0.092	730	10.34	0.22	0.22
7400	104.8	3.29	31.9	5.6	0.06	0.047	568	8.04	0.077	0.12
5300	75.1	2.41	31.2	6.4	0.08	0.064	654	9.26	0.12	0.17
538*	7.62	0.39	19.54	9.99	0.513	0.16	195	2.76	0.36	0.38
1024*	14.50	0.59	24.58	10.22	0.339	0.11	312	4.42	0.30	0.31
1804*	25.55	0.94	27.18	8.95	0.213	0.064	412	5.84	0.23	0.21
2060*	29.18	1.06	27.53	8.54	0.189	0.057	437	6.19	0.21	0.19
1032*	14.62	0.60	24.36	10.04	0.333	0.10	319	4.52	0.31	0.29
2078*	29.43	1.06	27.77	8.61	0.189	0.057	432	6.12	0.21	0.19
AERATOR No. 2										
1470	20.82	0.76	27.40	10.03	0.197	0.20	786	11.13	0.53	0.44
1000	14.16	0.57	24.85	10.51	0.263	0.26	613	8.68	0.61	0.54
850	12.04	0.52	23.15	10.25	0.288	0.28	549	7.78	0.65	0.55
690	9.77	0.45	21.73	10.34	0.333	0.33	485	6.87	0.70	0.61
535	7.58	0.39	19.43	9.93	0.385	0.38	399	5.65	0.75	0.65
2090	29.60	1.00	29.60	9.45	0.150	0.15	861	12.20	0.41	0.36
3300	46.74	1.48	31.58	8.29	0.101	0.10	941	13.33	0.29	0.26
7400	104.8	2.86	36.6	6.9	0.05	0.052	868	12.3	0.12	0.15
5300	75.1	2.10	35.8	7.9	0.07	0.071	914	12.9	0.17	0.20
538*	7.62	0.39	19.54	9.99	0.385	0.15	228	3.23	0.42	0.37
1024*	14.50	0.58	25.01	10.48	0.259	0.10	352	4.99	0.34	0.30
1804*	25.55	0.88	29.04	9.88	0.170	0.066	463	6.56	0.26	0.23
2060*	29.18	0.98	29.77	9.60	0.153	0.059	496	7.03	0.24	0.21
1032*	14.62	0.58	25.20	10.57	0.259	0.10	348	4.93	0.34	0.31
2078*	29.43	0.99	29.73	9.54	0.152	0.059	492	6.97	0.24	0.21
AERATOR No. 3										
1470	20.82	0.73	28.52	10.66	0.137	0.19	775	10.98	0.53	0.45
1000	14.16	0.56	25.29	10.79	0.179	0.25	587	8.31	0.59	0.54
850	12.04	0.51	23.61	10.55	0.196	0.28	546	7.73	0.64	0.56
690	9.77	0.45	21.72	10.34	0.222	0.31	476	6.74	0.69	0.59
535	7.58	0.39	19.43	9.93	0.256	0.36	386	5.47	0.72	0.63
2090	29.60	0.93	31.83	10.54	0.108	0.16	846	11.98	0.40	0.40
3300	46.74	1.33	35.14	9.73	0.075	0.11	932	13.20	0.28	0.30
538	7.62	0.39	19.54	9.99	0.256	0.36	395	5.59	0.73	0.63
1024	14.50	0.57	25.45	10.76	0.175	0.25	604	8.56	0.59	0.53
1804	25.55	0.83	30.79	10.79	0.120	0.17	791	11.20	0.44	0.43
2060	29.18	0.91	32.06	10.73	0.110	0.16	832	11.78	0.40	0.40
1032	14.62	0.58	25.20	10.57	0.172	0.24	602	8.53	0.58	0.52
2078	29.43	0.92	31.99	10.65	0.109	0.16	832	11.78	0.40	0.40

* Asymmetric tests, with right hand side aeration tower closed. Aeration data made available by the owner "Companhia Paranaense de Energia - COPEL". The tests were carried out by COPEL and CEHPAR staff.

** C values based on actually measured pressures below the nappe.
Symmetric conditions - C₁ = 0.97; C₂ = 0.93 C₃ = 0.88
Asymmetric conditions - C₁ = 0.76; C₂ = 0.73

*** Value of B estimated by formula 5.

EMBORCAÇÃO SPILLWAY

Q	q	h	V	F _r	c/h	D/h*	Q _a	q _a	B	B _e
AERATOR No. 1										
452	7.73	0.44	17.6	8.5	0.68	0.45	306	5.23	0.68	0.64
504	8.62	0.46	18.7	8.8	0.65	0.43	343	5.86	0.68	0.64
556	9.50	0.48	19.8	9.1	0.63	0.41	375	6.41	0.67	0.64
614	10.5	0.51	20.6	9.2	0.59	0.39	399	6.82	0.65	0.62
672	11.5	0.54	21.3	9.3	0.55	0.37	424	7.24	0.63	0.61
1212	20.7	0.83	24.9	8.7	0.36	0.24	583	9.96	0.48	0.45
2824	48.3	1.66	29.1	7.2	0.18	0.12	721	12.3	0.26	0.26
AERATOR No. 2										
452	7.73	0.44	17.6	8.5	0.45	0.47	299	5.11	0.66	0.66
504	8.62	0.46	18.7	8.8	0.43	0.45	327	5.59	0.65	0.65
556	9.50	0.47	20.2	9.4	0.43	0.44	357	6.10	0.64	0.68
614	10.5	0.50	21.0	9.5	0.40	0.41	389	6.65	0.63	0.66
672	11.5	0.53	21.7	9.5	0.38	0.39	422	7.21	0.63	0.64
1212	20.7	0.78	26.5	9.6	0.26	0.26	615	10.5	0.51	0.51
2824	48.3	1.48	32.6	8.6	0.14	0.14	823	14.1	0.29	0.33

Aeration tests carried out by the owner "Companhia Energética de Minas Gerais - CEMIG", 1982.

* C₁ = 0.35; C₂ = 0.88 based on measured pressure values under the nappe.

AMALUZA SPILLWAY

Q	q	h	V	F _r	c/h	D/h*	Q _a	q _a	B	B _e
1.327	18.4	0.67	27.5	10.7	0.09	0.34	748	10.4	0.56	0.64
920	12.8	0.48	26.7	12.3	0.125	0.47	680	9.44	0.74	0.85
854	11.9	0.45	26.4	12.6	0.133	0.50	671	9.35	0.79	0.90
879	12.2	0.46	26.5	12.5	0.130	0.49	671	9.32	0.76	0.88
587	8.15	0.32	25.1	14.2	0.187	0.71	551	7.65	0.94	1.19
333	4.62	0.21	21.9	15.3	0.286	1.07	416	5.78	1.25	1.60
168	2.33	0.12	19.4	17.9	0.500	1.89	320	4.44	1.90	2.47
88	1.22	0.07	17.4	21.0	0.85	3.23	275	3.82	3.12	3.77

Aeration tests carried out by the owner "Instituto Ecuatoriano de Electrificación - INECEL", July, 1984.

C = 1.13, estimated from the air duct geometry - bellmouth entrances at both sides and intermediate vertical towers.

COLBUN SPILLWAY

Q	q	h	V	F _r	c/h	D/h*	Q _a	q _a	B	B _e
AERATOR No. 1										
290	4.9	-0.33	-15.0	-8.4	-0.76	-0.43	233	3.9	0.80	0.62
1360	22.8	0.98	23.3	7.5	0.26	0.14	475	8.0	0.35	0.30
3260	54.7	2.15	25.3	5.5	0.12	0.064	353	5.9	0.11	0.15
AERADOR No. 2										
290	5.4	-0.27	-20.0	-12.2	-1.08	-0.59	252	4.7	0.87	0.96
1360	25.2	0.83	30.2	10.6	0.30	0.19	501	9.3	0.37	0.45

Aeration tests carried out by ENDESA, Chile, 1987.

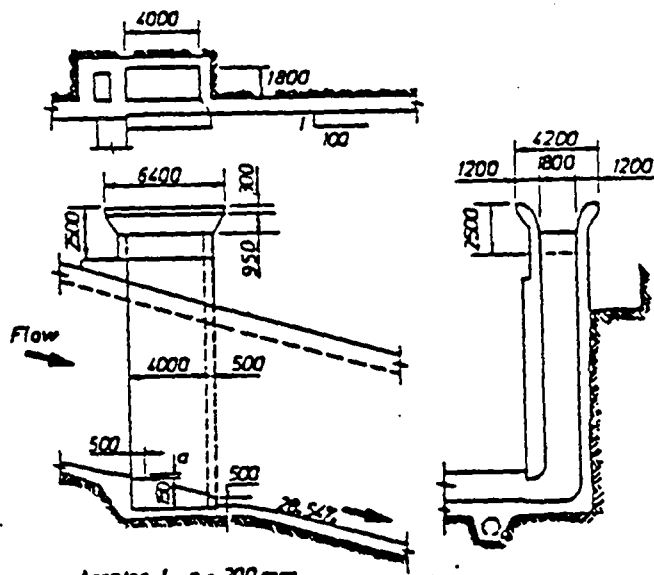
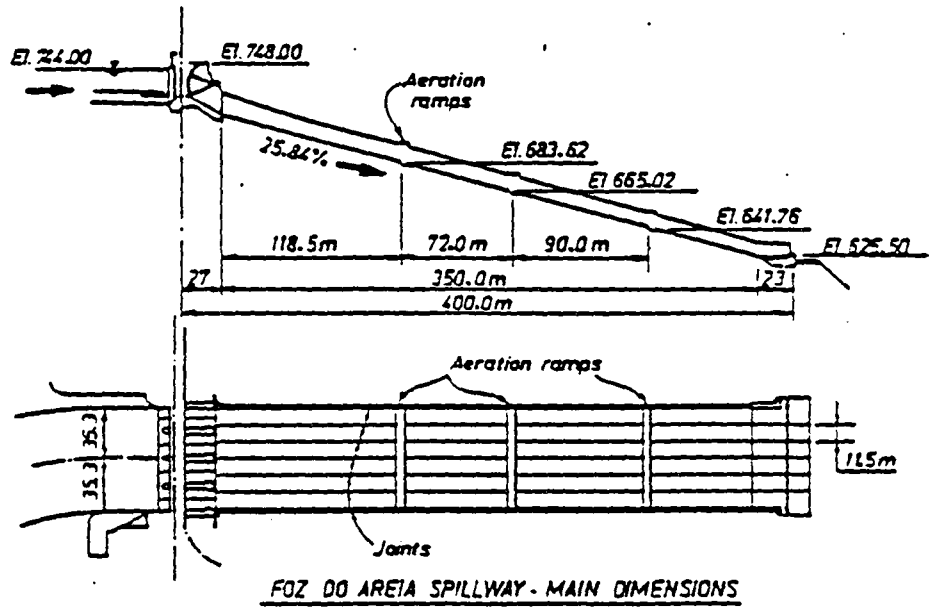
*C = 0.95 estimated in analogy to Foz do Areia results.

TARBELA, TUNNEL 3 OUTLET

Q	q	h	V	F _r	c/h	D/h*	Q _a	q _a	B	B _e
Res. el. 1500'										
1404	255	7.33	34.8	4.1	0.02	0.028	140	25.5	0.1	0.072
563	115	2.44	47.1	9.6	0.06	0.085	197	40.2	0.35	0.26
Res. el. 1390'										
1178	214	7.33	29.2	3.4	0.02	0.028	100	18.2	0.085	0.06
476	98	2.44	39.8	8.1	0.06	0.085	133	27.4	0.28	0.23
Res. el. 1300'										
953	173	7.33	23.6	2.8	0.02	0.028	42.9	7.8	0.045	0.05
391	80	2.44	32.7	6.7	0.06	0.085	89.9	18.4	0.23	0.20

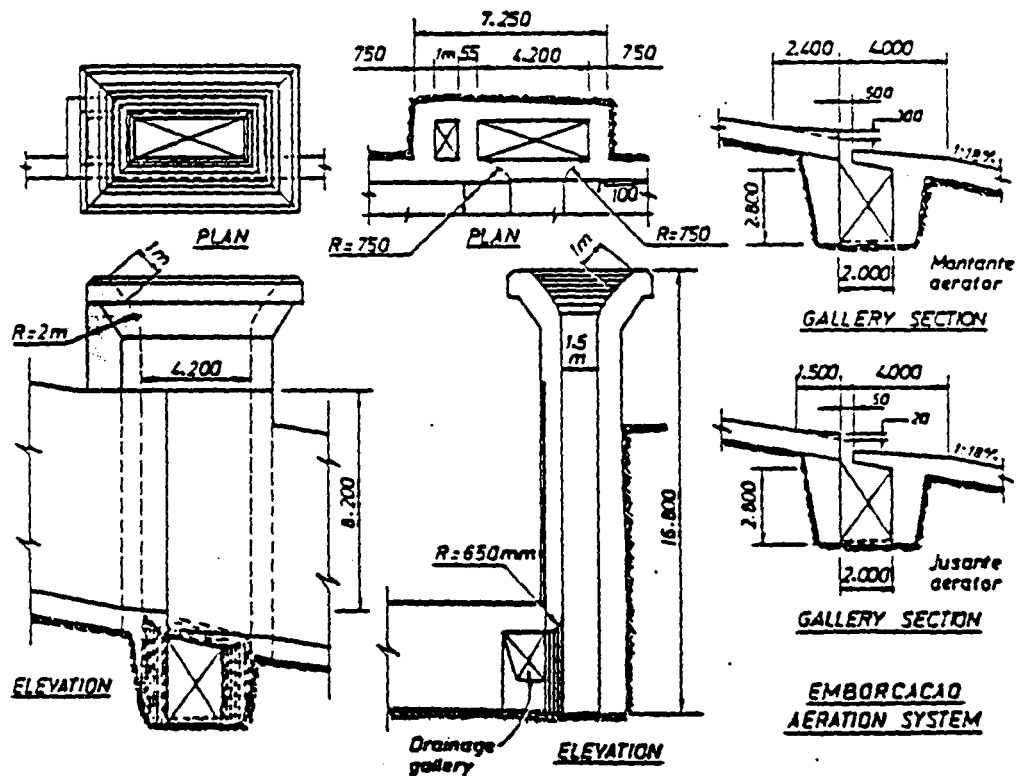
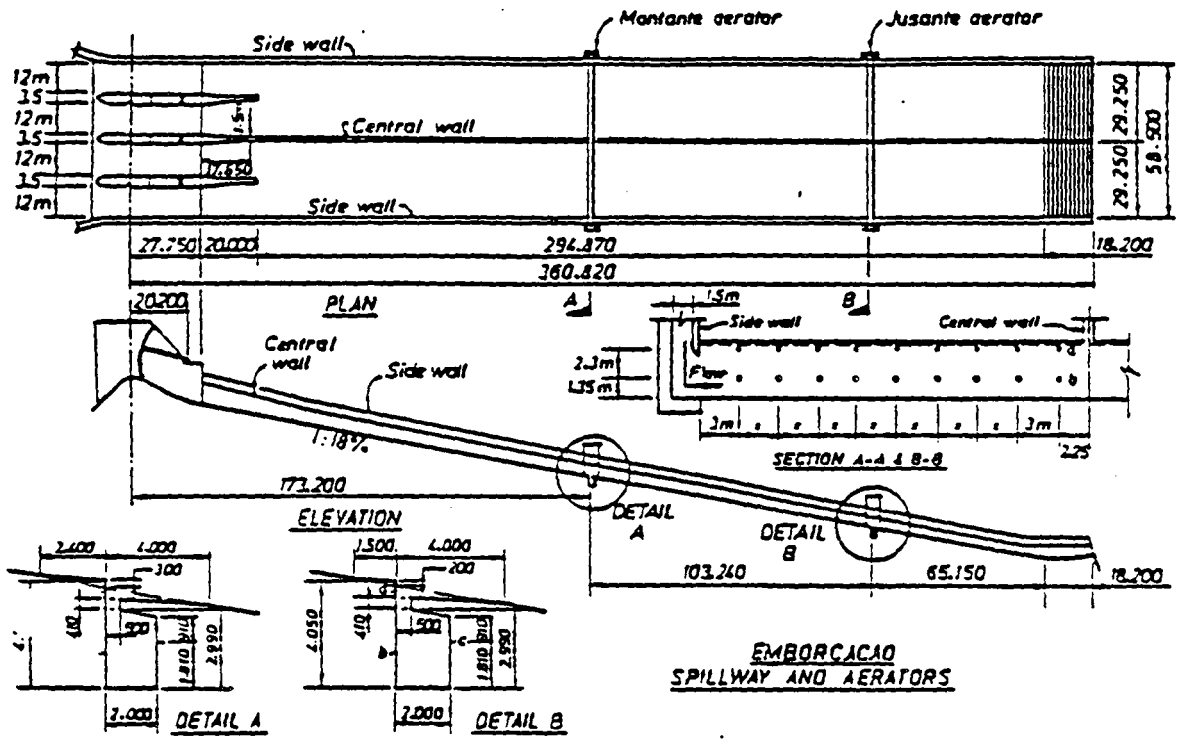
Tarbela data was based on values plotted on reference 2, discharges being estimated from the tunnel dimensions, reservoir elevation and gate opening.

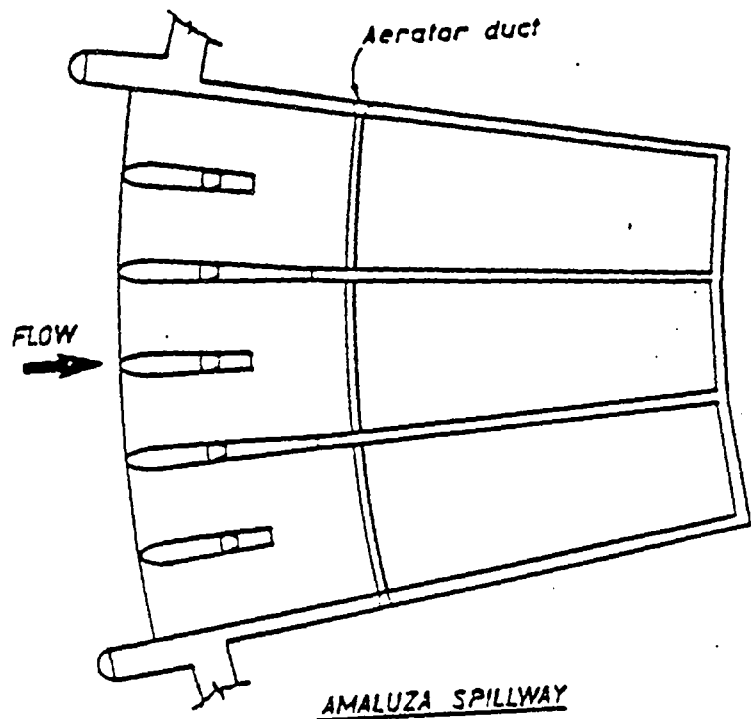
*C = 0.71, postulating uniform pressure distribution under the nappe.



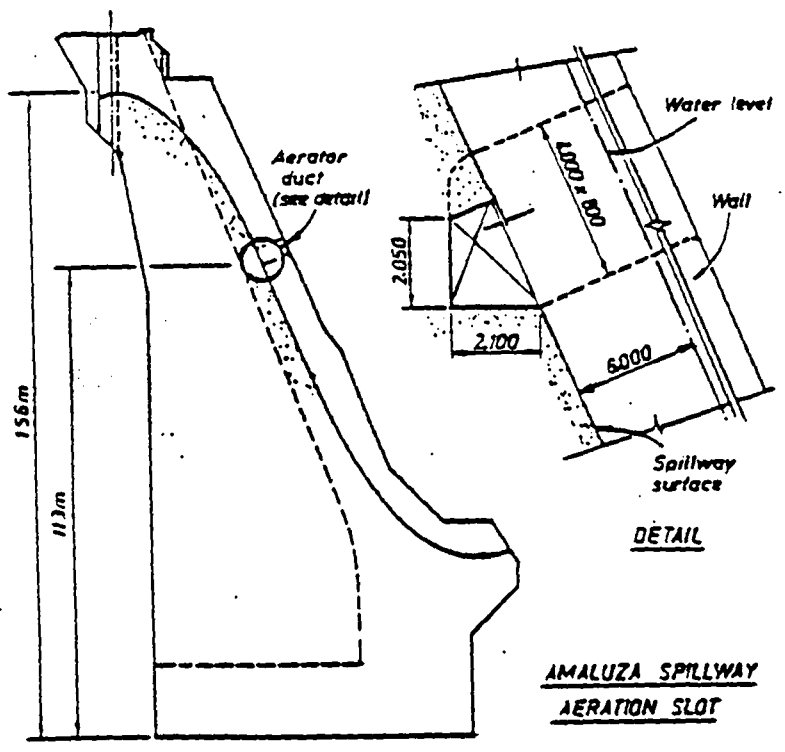
- Aerator 1 a = 200 mm
- .. 2 a = 150 mm
- .. 3 a = 100 mm

**FOZ DO AREIA
AERATION SYSTEM**



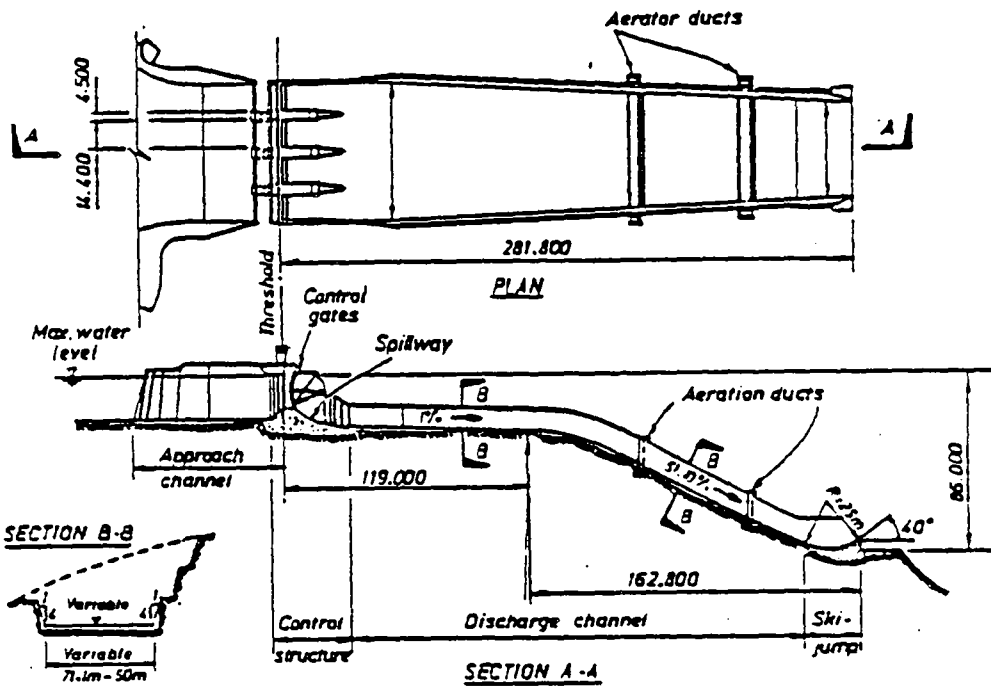


AMALUZA SPILLWAY
General Plan

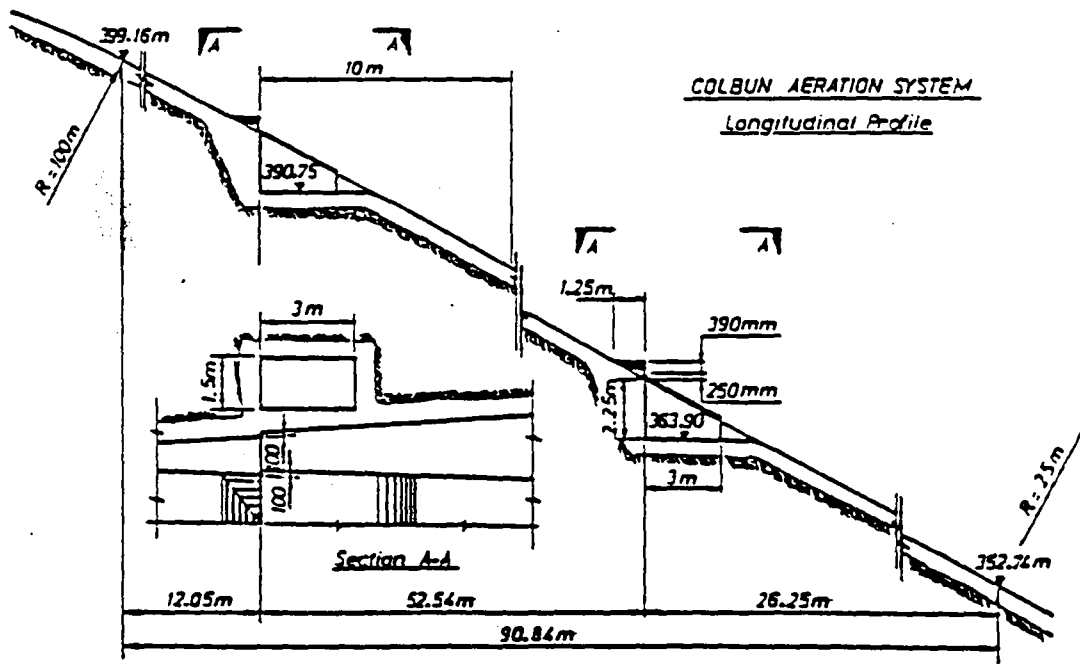


DETAIL

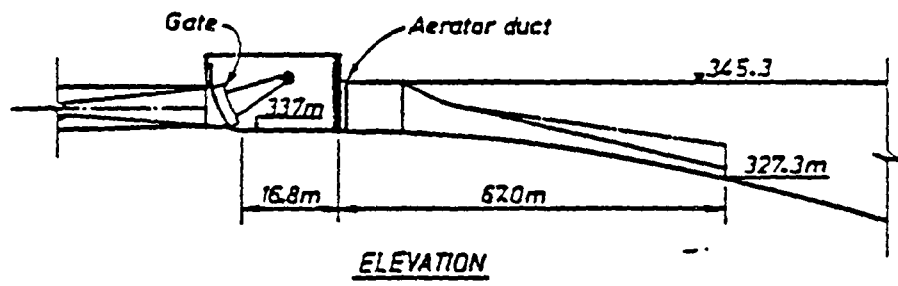
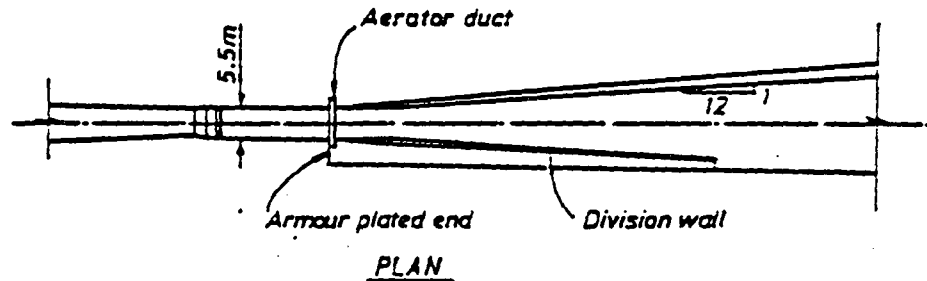
AMALUZA SPILLWAY
AERATION SLOT



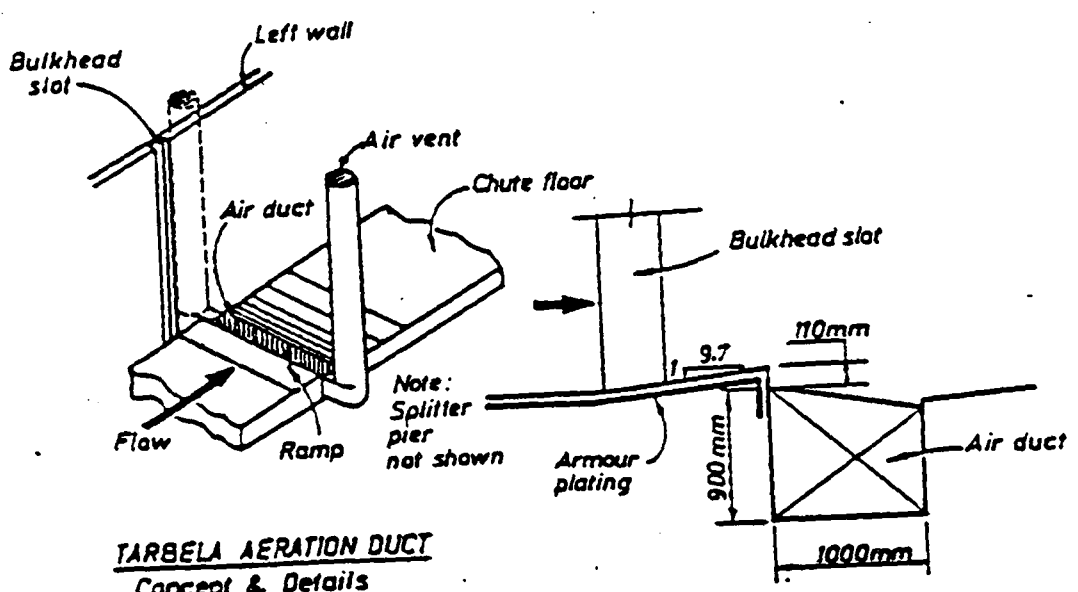
COLBUN SPILLWAY AND AERATORS



COLBUN AERATION SYSTEM
Longitudinal Profile



TARBELA BOTTOM OUTLET



TARBELA AERATION DUCT
Concept & Details

INDEX

Aeration	
local	1.6, 2.2, 2.3
natural	1.5, 3.1
self	1.5
systems	1.4, 1.12, 4.1
Aerator	
inlet duct	4.20
jet trajectory	4.8, 4.14
location	4.22
main duct	4.16
model scale effects	4.15
model studies	4.10, 4.15, 5.1
pressure coefficient	4.11, 5.1
pressure gradient term	4.11
shapes	4.19, 4.22
spacing	4.23
supply system	4.16
Aerator examples	
Amaluza	5.1
Clyde dam	4.1
Colbun dam	5.1
Emboracão	5.1
Foz do'Areia	5.1, 5.2
Aerators	4.1, 4.5
Aerator zones of flow	
aeration zone	4.5
approach zone	4.5
ramp zone	4.6
reattachment zone	4.5
redistribution zone	4.9
transition zone	4.5
Air	
bubbles	1.15, 1.26, 1.27
chamber	1.3
concentration	3.7, 4.14, 5.4
demand	1.2
de-entrainment	1.3, 1.15
duct	4.6, 4.16, 4.20
entrainment	1.2, 1.15, 1.17, 2.7, 2.13, 2.14, 2.23
entrainment limit	1.17
escape	2.31
in hydraulic jump	2.24
in impinging jets	2.8, 2.9
in solution	1.4
supply limit	1.19
supply system	1.12
suspended	1.6
transport	1.2, 2.31
transport capacity	1.15
Amaluza Aerator	5.1

Blowback	1.14
Blowout	1.14
Bubbles	
cloud	1.26, 1.27
drag coefficient	1.23, 1.24, 1.25
formation	1.20
entrapment	1.20
rise velocity	1.15
size	1.21, 1.22, 2.24, 3.2
slip velocity	1.23, 1.24, 1.25
transport	1.20
water velocity, induced by	1.31
Colbun Aerator	5.1
Cavitation	3.1, 4.1, 4.2, 4.5
cavitation parameter	4.2, 4.3
Clyde Dam	5.1
Compression wave	4.5
Concrete	
cavitation	4.24
quality	4.23
Conduit	1.16
Critical Velocity	2.11
Crossflow	1.27, 1.28, 1.29
Detrainment	1.3, 1.15
Drag coefficient	1.23, 1.24, 1.25
Drop structures	2.11
Entrainment	1.2, 1.15, 1.17, 2.7, 2.13, 2.14, 2.23
Foam	1.8
Foz do Areia aerator	5.1, 5.2
Hydraulic Jumps	1.9, 1.10, 1.16, 2.2, 2.3, 2.6, 2.23, 2.29
Hydraulic	
models	2.28
free surface models	2.27
Inception	
limit	1.17, 2.4
point of	2.4

Jets		
	plunging	1.7, 1.8, 2.4, 2.11, 2.15, 2.28
	break up	2.11, 2.12, 4.8
	trajectory	4.8
Mass Transfer		2.25
Oxygenation		2.26
Oxygen Transfer		2.2, 2.17, 2.25
Plunge Pools		2.18, 2.19, 2.20, 2.21
Pressure		
	duct under pressure	5.3
	subatmospheric	1.19
Reoxygenation		1.4, 2.2, 2.19, 2.25
Similarity		
	aerator	4.10
	air transport	2.31
	escape	2.31
	oxygen transfer	2.31
Siphons		1.10, 2.8
Spillways		1.11, 1.14, 1.32, 4.1, 5.1
	air entrainment function	3.13, 3.14
	Aviemore	4.2
	boundary layer	3.1, 3.4, 3.7, 4.6
	flow depth	3.8
	friction factor	3.8, 3.9, 3.11
	roughness	3.1, 3.12
	slope	3.3, 3.4, 3.5, 3.6
	turbulence	3.2
	uniform flow region	3.12
	varied flow region	3.13, 3.15
Transport capacity		1.6
Turbulence		1.8, 1.30, 2.6, 2.8, 2.11, 2.28 2.29, 3.2, 4.6, 4.7, 4.10, 4.11
Velocity distribution		3.11
Vortices		1.8, 1.11, 1.13, 3.1, 3.14
Wakes		1.11
Water		
	polluted	2.18
	quality	2.31
Weirs		1.6, 2.11, 2.15, 2.16
	oxygenation	2.22